LUND UNIVERSITY

Streptococcus pyogenes evades adaptive immunity through specific IgG glycan hydrolysis

Nägeli, Andreas; Bratanis, Eleni; Karlsson, Christofer; Shannon, Oonagh; Kalluru, Raja; Linder, Adam; Malmström, Johan; Collin, Mattias

ARTICLE

Streptococcus pyogenes evades adaptive immunity through specific IgG glycan hydrolysis

Andreas Naegeli, Eleni Bratanis, Christofer Karlsson⬤, Oonagh Shannon, Raja Kalluru, Adam Linder, Johan Malmström⬤, and Mattias Collin⬤

Streptococcus pyogenes (Group A streptococcus; GAS) is a human pathogen causing diseases from uncomplicated tonsillitis to life-threatening invasive infections. GAS secretes EndoS, an endoglycosidase that specifically cleaves the conserved *N*-glycan on IgG antibodies. In vitro, removal of this glycan impairs IgG effector functions, but its relevance to GAS infection in vivo is unclear. Using targeted mass spectrometry, we characterized the effects of EndoS on host IgG glycosylation during the course of infections in humans. Substantial IgG glycan hydrolysis occurred at the site of infection and systemically in the severe cases. We demonstrated decreased resistance to phagocytic killing of GAS lacking EndoS in vitro and decreased virulence in a mouse model of invasive infection. This is the first described example of specific bacterial IgG glycan hydrolysis during infection and thereby verifies the hypothesis that EndoS modifies antibodies in vivo. This mechanisms of immune evasion could have implications for treatment of severe GAS infections and for future efforts at vaccine development.

Introduction

Streptococcus pyogenes (group A streptococcus; GAS) is a human pathogen causing a diverse range of diseases. GAS can cause mild infections such as tonsillitis and impetigo but also severe diseases such as streptococcal toxic shock syndrome, necrotizing fasciitis, and erysipelas (Walker et al., 2014). Furthermore, repeated and/or untreated GAS infections can trigger serious postinfectious immune-mediated disorders, including acute poststreptococcal glomerulonephritis, acute rheumatic fever, and rheumatic heart disease (Walker et al., 2014). With a prevalence of ≥18 million severe cases, leading to approximately half a million deaths worldwide annually, as well as >700 million annual cases of mild infections (Carapetis et al., 2005), GAS infections are a large public health burden.

Protective immunity toward GAS is generally poor, and recurrent infections are not uncommon, especially in children (St Sauver et al., 2006). This is despite the fact that most people do in fact raise an adaptive immune response and exhibit high titers of IgG antibodies toward different GAS antigens (Todd, 1932; Lancefield, 1962; O'Connor et al., 1991; Åkesson et al., 2004). The reason for the lack of protection is not entirely understood but can in part be attributed to the large number of different GAS serotypes and the surface antigen variability this entails (McMillan et al., 2013). GAS is also able to counteract adaptive immunity by specifically impairing IgG function. This can be mediated by nonimmune IgG binding to Fc (fragment crystallizable)–binding proteins on the streptococcal surface such as the M and M-related proteins (Åkesson et al., 1990, 1994) or through specific degradation of the IgGs themselves. GAS secretes, for example, the IgG-degrading enzyme of *S. pyogenes* (IdeS), an IgG-specific protease that is able to cleave the antibody in the hinge region, separating the antigen-binding Fabs from the effector function–promoting Fc region (von Pawel-Rammingen et al., 2002).

GAS is further able to degrade IgGs by secretion of the endoglycosidase of *S. pyogenes* (EndoS). This enzyme cleaves the conserved Fc *N*-glycan from IgGs with great specificity (Collin and Olsén, 2001; Fig. 1 A). This glycan is situated at the interaction surface between the IgG and Fc receptors (Subedi and Barb, 2015, 2016) as well as the complement system (Burton, 1985) and is therefore ideally located to influence IgG effector function. While an antibody's specificity is determined by the Fab regions, the Fc region determines which effector functions are elicited, and the structure of the Fc glycan has been shown to be crucial in the regulation of this process (Burton and Dwek, 2006). For example, IgGs lacking core fucosylation exhibit increased affinity for FcγRIIIA and are therefore significantly more potent in eliciting antibody-dependent cellular cytotoxicity (Shinkawa et al., 2003; Okazaki et al., 2004). Furthermore, the degree of galactosylation of the Fc glycan influences an IgG's ability to activate the complement system (Peschke et al., 2017).

Faculty of Medicine, Department of Clinical Sciences, Division of Infection Medicine, Lund University, Lund, Sweden.

Correspondence to Mattias Collin: mattias.collin@med.lu.se;   A. Naegeli's present address is Genovis AB, Lund, Sweden;   R. Kalluru's present address is Department of Pathology, Stanford University School of Medicine, Stanford, CA.
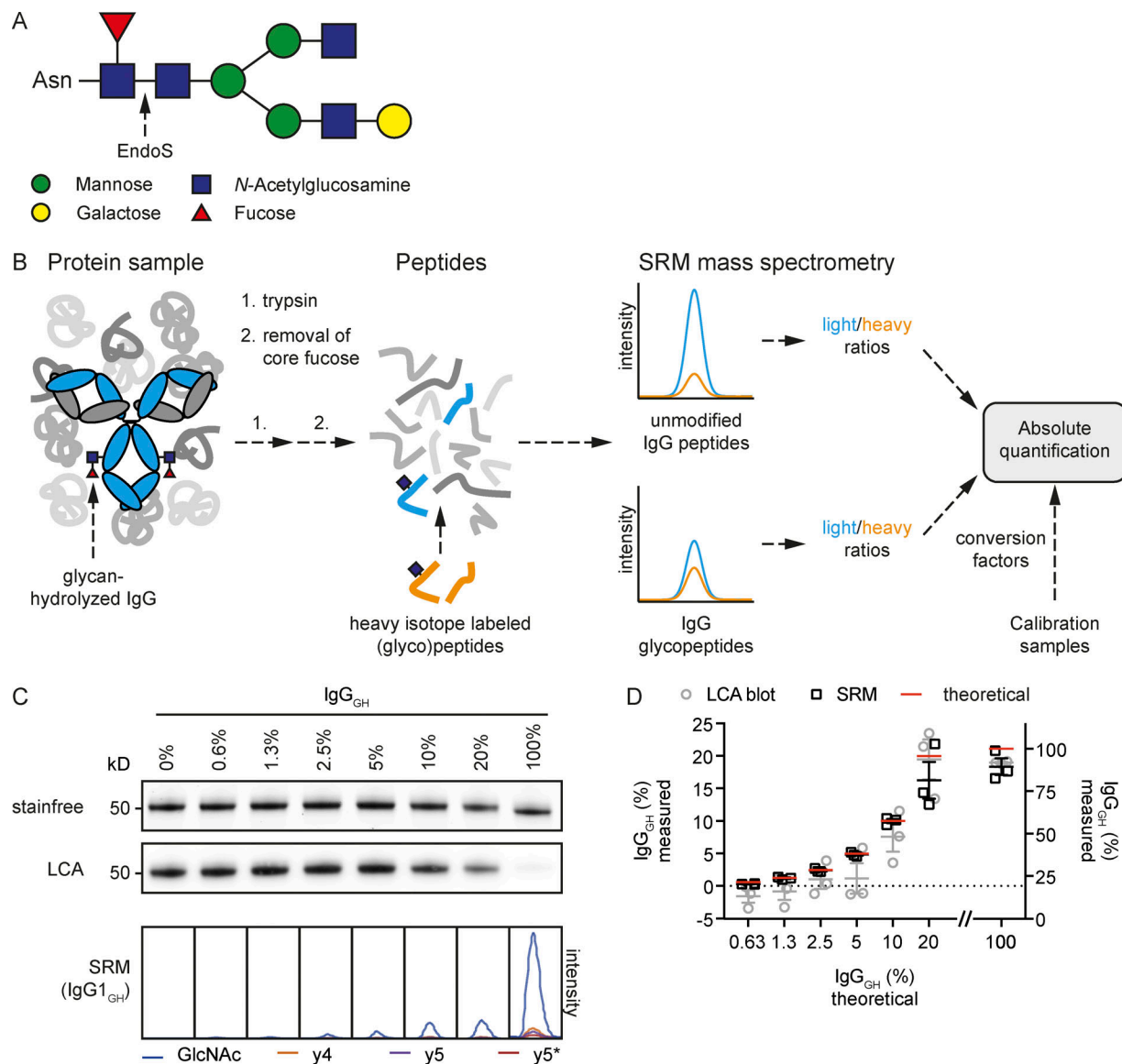
Figure 1. Targeted MS to quantify IgG glycan hydrolysis. (A) Typical *N*-glycan structure found on N297 of human IgG antibodies. The arrow marks the EndoS cleavage site in the chitobiose core of the glycan. The EndoS reaction product is an IgG carrying either a single GlcNAc or a GlcNAc-Fucose disaccharide, depending on the core fucosylation status of the antibody. **(B)** Overview of the SRM-MS method. Complex protein samples are digested to peptides using trypsin, and potential core fucosylation is removed using α-fucosidase. The resulting peptide samples are spiked with heavy isotope–labeled (glyco)peptide standards corresponding to both subclass-specific IgG glycopeptides modified with a single GlcNAc residue, as well as subclass-specific unmodified peptides. This peptide mixture is analyzed by SRM-MS, resulting in light/heavy ratios for each of the peptides of interest. The absolute amount (concentration) of each IgG subclass as well as the amount of IgG$_{GH}$ is derived from the obtained ratios, using conversion factors determined from a defined set of standard samples. **(C and D)** Validation of SRM-MS quantitative accuracy. A set of plasma samples with defined percentages of IgG$_{GH}$ was prepared by dilution of EndoS-treated plasma with untreated control plasma. The samples were analyzed separately in triplicate by SDS-PAGE (stain free)/LCA (the lectin LCA recognizing the intact glycan) blotting and SRM-MS. Raw data from both methods is shown in C. For the SRM method, the chromatograms originating from the glycan-hydrolyzed IgG1 glycopeptide are shown, each transition in a different color. The asterisk denotes a fragment ion that has undergone a neutral loss of the GlcNAc modification. The degree of IgG glycan hydrolysis in the standard sample set was quantified using both methods (D). The red line marks the theoretical value, and the measured values are depicted in gray circles (LCA blot) and black boxes (SRM). The means and standard errors are plotted, and each individual data point is marked with a circle or box. The first six values are plotted on the left z axis, and the final 100% IgG$_{GH}$ sample on the right y axis.

Consequently, IgG antibodies lacking the Fc glycan fail to bind to most Fc receptors and are unable to activate the complement system (Nose and Wigzell, 1983; Lux et al., 2013). Despite the accumulating evidence that antibody glycans are instrumental in regulating antibody effector functions, very little is known about the role of antibody glycosylation during infections and if it contributes to the outcome of disease. However, a few important recent studies have suggested that IgG glycosylation status influences whether HIV infection is controlled (Ackerman et al., 2013; Alter et al., 2018) and whether *Mycobacterium tuberculosis* infection is active or latent (Lu et al., 2016).

Due to this functional importance of the Fc *N*-glycan, its hydrolysis by EndoS leads to impaired IgG effector functions such as Fc receptor binding and complement activation in vitro (Collin et al., 2002; Allhorn et al., 2008a; Lux et al., 2013). This would intuitively suggest a role for EndoS in evasion of adaptive immunity through perturbation of protective IgG responses. However, studies on the influence of EndoS on GAS pathogenesis have so far been few and inconclusive. They were unable to demonstrate under which conditions EndoS is expressed and active and had to rely on overexpression or addition of recombinant enzyme to manifest a virulence phenotype (Collin et al., 2002; Sjögren et al., 2011). These efforts at elucidating the contribution of EndoS to GAS virulence have been hampered by the difficulty of finding relevant model systems and the lack of a sensitive analytical approach to quantify EndoS activity in complex systems.

We therefore wanted to take a different approach by first characterizing the effect of EndoS on the host's IgG glycosylation in vivo during the course of natural GAS infections in human patients, and then use these results to set up a relevant model system able to show how EndoS affects the host's IgG response and how this contributes to GAS virulence. This necessitates an assay that is robust, specific, and sensitive enough to be able to quantify the glycosylation state of IgG in complex patient samples. We chose to employ selected reaction monitoring (SRM), a targeted mass spectrometry (MS) approach that is uniquely suitable for this type of analysis, as it allows for the quantification of predefined target molecules directly from highly complex samples. SRM is based on precursor peptide ion selection, fragmentation through collision, and detection of selected peptide fragment ions in a triple-quadrupole mass spectrometer. Precursor/fragment pairs, so-called transitions, are chosen that are unique to the molecule to be detected (i.e., the EndoS reaction products), and data are acquired only for these defined targets (Lange et al., 2008). In previous studies, proteins with concentrations as low as 300 ng/ml have been reliably quantified out of crude human plasma preparations (Anderson and Hunter, 2006; Addona et al., 2009), and SRM has also been used successfully for quantification of the different glycan structures on IgG directly from serum samples (Hong et al., 2013).

We employed SRM-MS to quantitatively assess the EndoS-mediated IgG glycan hydrolysis in samples from natural GAS infections in humans. We used these findings to set up relevant in vitro assays and animal models to demonstrate the importance of EndoS-mediated antibody modification in evasion of adaptive immunity and therefore GAS virulence.

Results

A targeted MS approach for quantitative analysis of IgG glycan hydrolysis

To assess the effect of EndoS on IgG glycosylation during streptococcal infections in vivo, we first needed an assay powerful enough to allow us to quantify the EndoS reaction products directly from very complex samples such as patient material (plasma, wound swabs, or throat swabs). Previous attempts at measuring EndoS activity relied on SDS-PAGE (Collin et al., 2008; Sjögren et al., 2015) or analysis of released glycans by HPLC (Dixon et al., 2014). These methods lack sensitivity and specificity and/or are ill-suited for analysis of complex material. We therefore developed an SRM-MS method to specifically quantify the amount of glycan-hydrolyzed IgGs (IgG$_{GH}$). As EndoS cleaves within the chitobiose core of the IgG *N*-glycan (Fig. 1 A), it leaves the reducing end *N*-acetylglucosamine (GlcNAc) residue attached to the protein (Collin and Olsén, 2001) and leads to the generation of a new IgG proteoform with a truncated glycan that is not detected in healthy individuals (Wuhrer et al., 2007; Pucić et al., 2011). Samples were digested with trypsin, and the peptides were treated with α-fucosidase to remove potential core fucosylations and end up with a single EndoS reaction product per IgG subclass. We defined SRM transitions for the tryptic peptides containing the glycosylation site of human IgG (IgG1, EEQYN(GlcNAc)STYR; IgG2, EEQFN(GlcNAc)STFR; IgG3, EEQYN(GlcNAc)STFR; and IgG4, EEQFN(GlcNAc)STYR) modified with a single *N*-linked GlcNAc residue. As the glycopeptides of IgG3 and IgG4 have the same precursor mass, we defined transitions that are in common and quantified both peptides together. To assess total IgG levels, previously developed SRM assays for quantification of each IgG subclass (Karlsson et al., 2017) were included. All the transitions are listed in Table S1. To determine the absolute amounts of IgG and IgG$_{GH}$, we synthesized heavy isotope–labeled standard peptides corresponding to the peptides we analyzed, which could be spiked into the samples to act as internal standards (Fig. 1 B). The method was calibrated using a defined human standard serum (Fig. S1 and Table S2) and validated by analyzing a set of human blood plasma samples with defined amounts of IgG$_{GH}$. For method comparison, the same samples were also analyzed by SDS-PAGE and *Lens culinaris* agglutinin (LCA) lectin blot (Fig. 1, C and D). The SRM method exhibited better precision and accuracy as well as a much lower detection limit. Especially for samples where the IgG$_{GH}$ content was low, as might be expected in clinical samples, the SRM method outperformed the SDS-PAGE assay. This, together with low sample requirements, a large dynamic range, and high analytical precision, made this method highly suitable for the analysis of complex patient materials.

IgG glycans are hydrolyzed during GAS tonsillitis

Tonsillitis is the most common form of GAS infection and is characterized by throat pain, fever, tonsillar exudates, and cervical lymph node adenopathy (Walker et al., 2014). To study the effects of EndoS on patient IgGs during such an infection, we obtained 59 throat swab samples from a total of 54 patients who sought medical attention for a sore throat (Fig. 2 A). 26 of the patients were diagnosed with GAS tonsillitis by rapid strep test and/or throat culture and were prescribed oral antibiotics. The other 28 patients exhibited a negative strep test and throat culture; therefore, the infection was suspected to be viral and left untreated. Five of the patients diagnosed with GAS tonsillitis were willing to return after antibiotic treatment, and an additional throat swab was collected for each of these (Fig. 2 A).
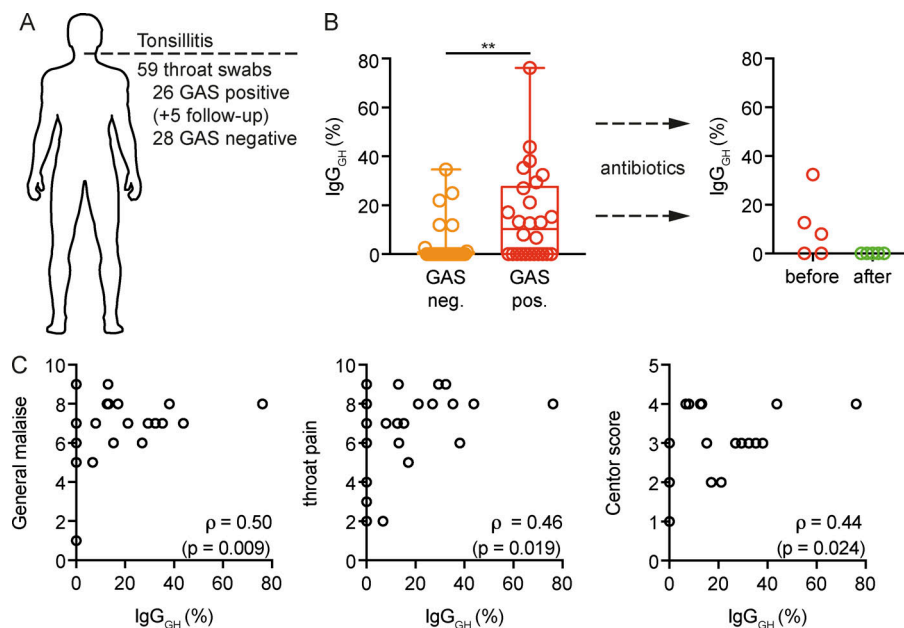
Naegeli et al.
Immune evasion through IgG glycan hydrolysis

Journal of Experimental Medicine 1617
https://doi.org/10.1084/jem.20190293

Figure 2. **IgG glycan hydrolysis during GAS tonsillitis. (A)** Overview of the collected throat swab samples from patients seeking medical attention for a sore throat. A total of 59 samples were taken from 54 different patients (26 GAS-positive tonsillitis, 28 GAS-negative tonsillitis). Follow up refers to additional samples that were taken from five of the GAS tonsillitis patients after antibiotic treatment. **(B)** Percentage of IgG_{GH} as determined by SRM-MS analysis of tonsillar swabs from patients with, either GAS-negative (orange) or GAS-positive (red) tonsillitis. The boxes represent the 25th to 75th percentiles, with the median depicted as a line in the middle. The whiskers reach from the smallest to the largest data point, all of which are marked as circles. Glycan hydrolysis of the individual subclasses is shown in Table S3. The glyco-peptides from IgG3 and IgG4 could not be measured in these samples due to interfering background and were omitted from this analysis. Data were analyzed using a Mann–Whitney U test (not significant [ns], P > 0.05; **, P < 0.01). **(C)** The tonsillitis patients were asked to grade their general malaise (left) and throat pain (middle) on a scale from 0 to 10, and the Centor score (right; Centor et al., 1981) was determined. These parameters were correlated to the IgG glycan hydrolysis measured in tonsillar swabs using SRM-MS. Correlation was analyzed according to Spearman.

We used SRM-MS to quantitatively analyze the levels of IgGs as well as their glycosylation status in these throat swab samples. We observed no difference between GAS-positive and GAS-negative patients in total IgG content or in the distribution of the four IgG subclasses (Table S3). However, the percentage of IgG_{GH}s was significantly higher in the GAS tonsillitis group, with glycan hydrolysis approaching 80% in one case (Fig. 2 B, left). This was no longer detectable in any of the samples taken after antibiotic treatment (Fig. 2 B, right). Furthermore, IgG glycan hydrolysis could be correlated to the grade of throat pain and the general malaise experienced by the patients, as well as their Centor scores (a clinical scoring system aimed at distinguishing GAS tonsillitis from viral infections; Centor et al., 1981; Fig. 2 C). Taken together, these results suggest that EndoS is expressed and active during acute GAS tonsillitis, but its effects quickly disappear upon therapeutic intervention.

IgG antibodies are deglycosylated systemically during GAS-induced sepsis

Sepsis is a state of systemic inflammation in response to an infection and the worst-case scenario in GAS infections (Walker et al., 2014). To address the effect of EndoS on patient IgG antibodies during invasive GAS infection leading to sepsis, we collected blood plasma from 32 patients suffering from sepsis of various degrees of severity as well as 12 healthy volunteers. 18 patients had confirmed GAS infections, whereas the other 14 suffered from various other bacterial infections (Fig. 3 A and Table S3). All the sepsis patients were ranked according to the degree of severity of their condition (sepsis, severe sepsis, or

septic shock). We used our SRM method to determine IgG levels and glycosylation state in blood plasma (Fig. 3 B). The total IgG levels were not significantly different between the groups (Fig. 3 B), and no appreciable amounts of IgG_{GH} could be detected in any of the plasma samples from the control groups (healthy or non-GAS sepsis). The same was true for milder cases of GAS-induced sepsis. However, the plasma of five of six GAS patients suffering from septic shock contained significantly increased amounts of IgG_{GH} (≤1 mg/ml in the most severe case; Fig. 3 B).

As we observed large differences in IgG glycan hydrolysis, even among the septic shock patients, we hypothesized that differential expression of EndoS among the different GAS strains infecting these patients could account for part of the observed variance. We were able to obtain six GAS isolates from the blood cultures of these patients and analyzed the ability of these strains to secrete EndoS into the culture medium in vitro. Three isolates from severe sepsis patients and three from septic shock patients (Fig. 3 C, patients 1, 2, and 3) could be obtained. The strains exhibited large variability in EndoS expression as well as different levels of degradation of the EndoS protein. Strains secreting substantial amounts of EndoS and strains secreting almost no EndoS could be found in both groups. However, the amount of EndoS secreted by the isolates from the septic shock patients in vitro corresponded well with the amount of IgG_{GH} found in the corresponding patients' blood plasma. The isolate from the patient with no detectable IgG glycan hydrolysis in vivo did not secrete detectable amounts of EndoS in vitro, and conversely, the isolate from the patient with the highest in vivo glycan hydrolysis secreted the most EndoS
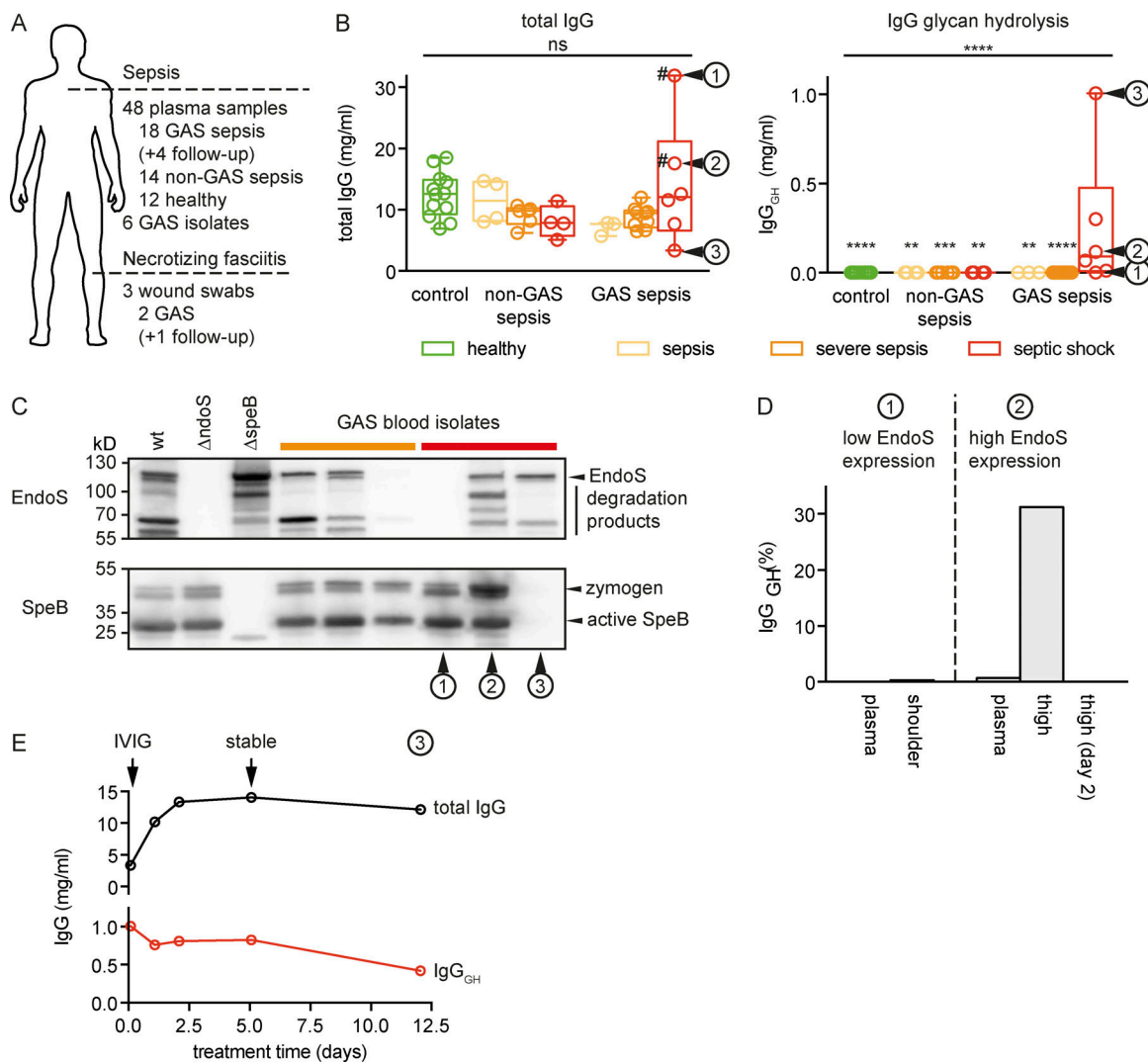
Naegeli et al.
Immune evasion through IgG glycan hydrolysis

Journal of Experimental Medicine
https://doi.org/10.1084/jem.20190293

1618

Figure 3. **IgG glycan hydrolysis during invasive GAS infection. (A)** Overview of the collected samples from sepsis patients. A total of 48 plasma samples, three wound swabs, and six GAS isolates was collected from 32 patients (18 GAS sepsis, 14 non-GAS sepsis) and 12 healthy control individuals. Follow up refers to four additional plasma samples that were taken from the same patient during the course of treatment and recovery. **(B)** Plasma concentration of total IgG (left) as well as the IgG_{GH} (right) as determined by SRM-MS. The patients are grouped according to infection state (healthy, non-GAS sepsis, GAS sepsis), as well as subgrouped according to severity of disease (sepsis, severe sepsis, septic shock). The boxes represent the 25th to 75th percentiles, with the median depicted as a center line. The whiskers reach from the smallest to the largest data point, all of which are marked as circles. Glycan hydrolysis of the individual subclasses is shown in Table S1. The P value of the overall comparison of all the groups (by Kruskal–Wallis test) as well as adjusted P values for the individual comparisons of the GAS septic shock group with each of the other groups are depicted (not significant [ns], $P > 0.05$; *, $P < 0.05$; **, $P < 0.01$; ***, $P < 0.001$; ****, $P < 0.0001$). Two patients (marked by #) had received IVIG treatment before the sample was drawn, affecting their total IgG concentrations. From three patients (marked 1–3), additional samples could be obtained, and their analysis is shown in the other panels of this figure. **(C)** Expression of EndoS and SpeB by clinical GAS isolates in vitro. Blood culture isolates from patients 1–3 as well as three patients from the GAS severe sepsis group were analyzed with respect to their ability of secrete EndoS (top) and SpeB (bottom) into the culture supernatant in vitro. The culture supernatants were analyzed by SDS-PAGE, followed by immunoblotting using rabbit antisera specific to EndoS and SpeB, respectively. AP1 (wild type) and isogenic *ndoS* and *speB* mutants were used as positive and negative controls, respectively. **(D)** Local versus systemic glycan hydrolysis. From patients 1 and 2, wound swab samples from the site of infection (patient 1, shoulder; patient 2, thigh) could be obtained and were analyzed by SRM-MS. The percentage of IgG_{GH} in the tissue as well as in plasma is shown. **(E)** IgG glycan hydrolysis over the course of infection. A series of plasma samples from patient 3 (starting at 2 h after admission until 12 d later) was analyzed using SRM-MS. The concentration of both total IgG (black) and IgG_{GH} (red) is shown. The arrows mark onset of IVIG treatment (4 h) and the time point when the patient was stable (5 d).

in vitro. The streptococcal cysteine protease SpeB is a secreted GAS virulence factor and has been shown to cleave the EndoS enzyme (Allhorn et al., 2008b). Strikingly, SpeB was absent from the culture supernatant of the GAS isolate from patient 3 (with the highest degree of plasma IgG glycan hydrolysis; Fig. 3 B) and consequently EndoS was largely intact.

The IgG glycan hydrolysis we observed in plasma reflects a systemic modification of IgG, which, due to the abundance of the antibody in circulation, necessitates large amounts of IgG to be deglycosylated to reach detectable levels. Locally, at site of infection, the effects of EndoS on the IgG pool are likely to be much more pronounced. To test this, we obtained wound swabs from

the infected tissue taken during surgery from two of the sepsis patients suffering from necrotizing fasciitis (patients 1 and 2). We analyzed them by SRM-MS to determine the degree of IgG glycan hydrolysis and compared the results with those previously obtained from analysis of plasma samples (Fig. 3 D). The samples originated from two of the patients whose GAS isolates we had analyzed for EndoS expression in vitro (Fig. 3 C, patients 1 and 2). One isolate did not secrete any detectable amounts (Fig. 3 C, patient 1), whereas the other one exhibited high EndoS expression (Fig. 3 C, patient 2). Accordingly, two very different patterns of IgG glycan hydrolysis could be observed in these patients (Fig. 3 D). The first patient showed no detectable IgG glycan hydrolysis in plasma and only a minor amount in the wound swab sample. The second patient, on the other hand, exhibited moderate IgG glycan hydrolysis in plasma (~0.7% hydrolyzed), and the amount of IgG$_{GH}$ was considerably higher in the wound swab sample from the same day (~30% hydrolyzed). This was no longer detectable in a sample from the same site that was taken during a second surgery the next day.

As we observed that local IgG glycan hydrolysis was transient, we wanted to determine how long-lasting the EndoS-mediated perturbation of the systemic IgG pool was. To this end, we obtained further plasma samples taken throughout the treatment and recovery periods (until 12 d after admission) from the patient exhibiting the highest amount of IgG$_{GH}$ in plasma (Fig. 3 B, patient 3). Shortly after admission (time point, 2 h), the patient presented with very low total IgG levels (3.3 mg/ml) and a high degree of IgG glycan hydrolysis (1 mg/ml). The patient was given intravenous immunoglobulin (IVIG) treatment, upon which the total IgG levels quickly normalized, but the concentration of IgG$_{GH}$ stayed high throughout the analyzed time interval and was still ~0.5 mg/ml at the 12-d end point (Fig. 3 E).

Taken together, these results suggest that EndoS is expressed and active during acute GAS infection in vivo. It is able to hydrolyze the glycans from a considerable portion of the IgG pool locally at the site of infection (both in tonsillitis and necrotizing fasciitis) as well as systemically in the most severe cases of GAS sepsis. This points toward an important role for EndoS in evasion of the immune defenses by perturbation of the host's IgG response.

EndoS is expressed during growth in saliva and protects GAS from phagocytic killing

While we were able to show that substantial IgG glycan hydrolysis takes place during GAS infections, the functional consequences of this process for GAS pathogenesis remained unclear and needed to be studied using appropriate model systems. As EndoS activity was measurable in the majority of samples from GAS tonsillitis patients, we attempted to set up a simplified in vitro model reminiscent of the conditions GAS encounters on an inflamed tonsil during such an infection. When GAS colonizes the throat, it would encounter saliva, an increasing amount of plasma proteins as inflammation leads to vascular leakage (Karlsson et al., 2017), and finally phagocytic immune cells trying to eradicate the bacteria. To approximate these conditions, we grew GAS strains 5448 and AP1 as well as their respective isogenic *ndoS* mutants in sterile-filtered saliva

supplemented with 5% serum and tested if EndoS would be expressed and active by SDS-PAGE. Based on electrophoretic mobility and/or LCA reactivity, both wild-type strains, but neither of the mutants, were able to deglycosylate the IgG pool under these conditions (Fig. 4, A and B). Strain AP1 further expressed IdeS (von Pawel-Rammingen et al., 2002), leading to proteolytic cleavage of IgG hinge in the culture supernatant. This resulted in a population of antibodies where the Fc glycans and at least half of the heavy chains had been cleaved (Fig. 4 A).

As IdeS and EndoS might be partially redundant, and strain 5448 secreted only EndoS without any detectable IdeS activity when grown in saliva, we used this strain to test the resistance of wild-type and *ndoS* mutant bacteria to phagocytic killing by human monocyte-derived macrophages (MDMs) and human polymorphonuclear leukocytes (PMNs) under the conditions described above. Deletion of the *ndoS* gene led to a small but significant increase in killing of the bacteria by both MDMs and PMNs (Fig. 4, C and D), and addition of recombinant EndoS reversed the phenotype. However, increased susceptibility to phagocytic killing was only observed when the assay was performed in the presence of serum containing GAS-specific IgGs (as determined by measuring the IgG response to streptococcal M1 protein by ELISA; Fig. S2). In the absence of specific IgGs, both mutant and wild type exhibited similar resistance to phagocytic killing. This indicates that EndoS confers increased resistance by neutralizing specific IgGs directed toward the pathogen and prevents them from mediating phagocytosis.

EndoS mutant GAS are less virulent in a mouse model of invasive GAS infection

To study the role of EndoS in neutralization of GAS-specific IgGs in more detail and determine its contribution to the outcome of streptococcal infection, we established a mouse model. As IdeS has no discernible activity on relevant subclasses of murine IgG (IgG1 and IgG2b; Nandakumar et al., 2007), we were able to use the more mouse-virulent strain AP1 for these experiments without confounding the results. Wild-type and *ndoS* mutant (Collin and Olsén, 2001) GAS were used to infect C57BL/6J mice subcutaneously, and both local (skin) and systemic (plasma and spleen) samples were taken 48 h after infection to determine bacterial loads as well as IgG glycan hydrolysis by SRM-MS (Fig. 5 A). An assay analogous to the one for human IgGs was developed to quantify murine IgG1 levels and its glycosylation status (Fig. S1). As EndoS does not exhibit any murine IgG subclass specificity (Albert et al., 2008), this can be used as an indicator for overall IgG glycan hydrolysis. When mice were infected with a wild-type GAS strain, IgG1 was almost completely deglycosylated locally, and ~30% glycan hydrolysis was observed systemically (Fig. 5 B). The animals exhibited a heterogeneous response to infection, with greatly varying degrees of severity observed. Consequently, the measured levels of IgG glycan hydrolysis also showed a large variance. We therefore tried to correlate IgG glycan hydrolysis and bacterial load in the skin samples and found a clear correlation between the two parameters (Spearman ρ = 0.95; Fig. 5 C). Mice infected with the *ndoS* mutant developed local and systemic signs of infection to a similar degree but showed no detectable IgG glycan hydrolysis
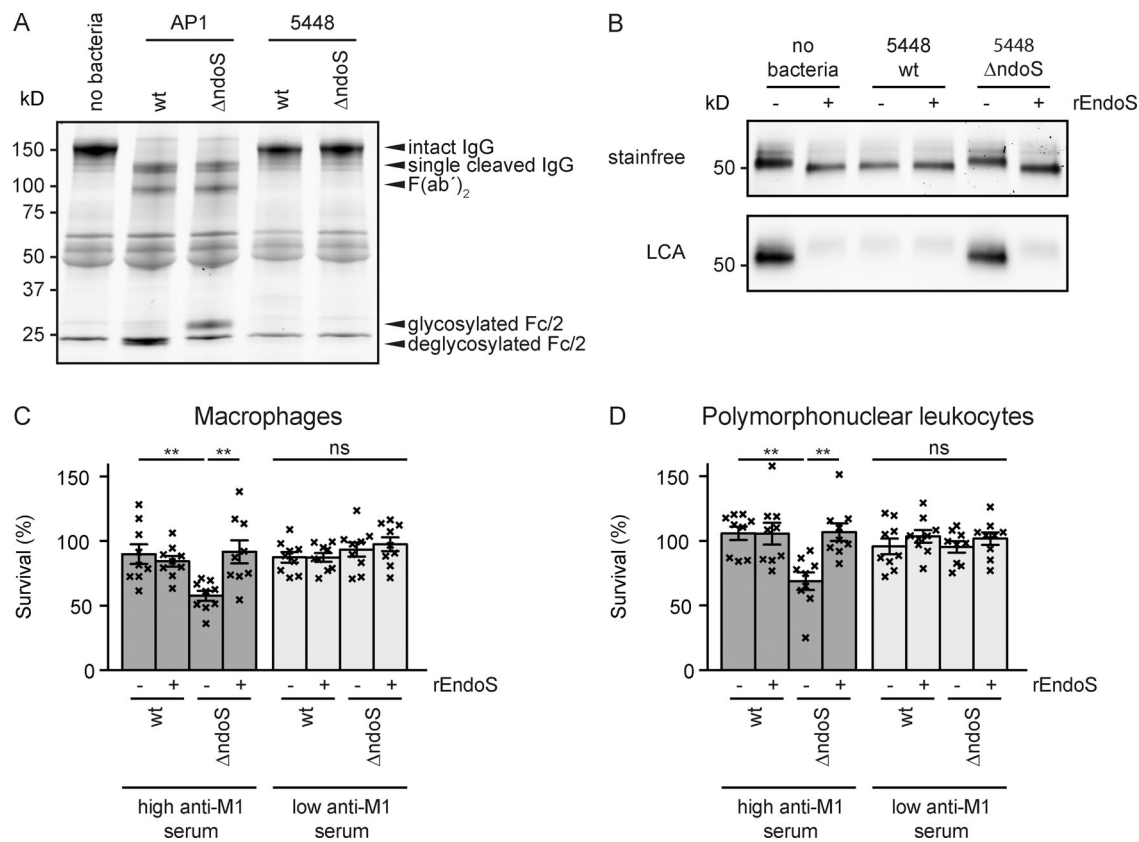
Naegeli et al.
Immune evasion through IgG glycan hydrolysis

Journal of Experimental Medicine
https://doi.org/10.1084/jem.20190293

1620

Figure 4. **EndoS confers resistance to phagocytic killing. (A)** GAS strains AP1, 5448, and their respective *ndoS* mutants were grown in human saliva supplemented with 5% serum, and the culture supernatants were analyzed by SDS-PAGE under nonreducing conditions. Note the lack of fully intact IgGs in the AP1 culture supernatants. **(B)** GAS 5448 and an isogenic *ndoS* mutant were grown in human saliva supplemented with 5% human serum. IgGs were purified by Protein G and analyzed by SDS-PAGE (top) and LCA blot (bottom). Addition of recombinant EndoS (rEndoS) was used to complement the mutation. **(C and D)** Saliva-grown GAS 5448 and an isogenic *ndoS* mutant were challenged with human MDMs (C) and human PMNs (D) in the presence of serum with a high (dark gray) or low (light gray) anti-M1 IgG response. Survival rates were determined by enumerating bacteria both in the initial inoculum and after incubation with the phagocytic cells. Data from three independent experiments with different cell donors (each performed in triplicate, total $n = 9$) were combined and analyzed using a Kruskal–Wallis test followed by Dunn's multiple comparison test (not significant [ns], $P > 0.05$; **, $P < 0.01$). The bar represents the mean, with the standard error depicted as error bars. Each individual data point is represented with a cross, showing the variability between the individual experiments and the replicates within the same experiment.

(Fig. 5 B). This indicates that EndoS is expressed and active during such an infection but does not confer any selective advantages under these nonimmune conditions.

As EndoS targets the adaptive immune response, its functional role during GAS infection is most appropriately studied in the context of adaptive immunity. We therefore immunized mice before infection through two injections with purified streptococcal M1 protein combined with adjuvant. After an IgG response to M1 was confirmed, the mice were infected subcutaneously, and survival was monitored for 5 d (Fig. 6 A). This immunization protocol led to a complete protection at an infectious dose of $2.5 × 10^5$ CFU, which could be overcome by increasing the dose to $2 × 10^7$ CFU (Fig. 6 B). The majority of mice infected with wild-type bacteria at that dose succumbed to the infection within 2–3 d (Fig. 6 B). On the other hand, >90% of the immunized mice infected with *ndoS* mutant bacteria survived the infection after recovering from an initial weight loss (Fig. 6 C, right, survival and weight loss). This profound difference in susceptibility to infection between wild-type and mutant could not be observed in animals that were mock-immunized by injection of adjuvant only, where both groups showed a similarly high mortality and weight loss (>90%; Fig. 6 C, left, survival and weight loss).

Discussion

IgG is a central molecule of the mammalian immune system. It provides a link between adaptive and innate immunity by specifically binding to antigens presented by a pathogen with its Fab regions and recruiting immune effectors with its Fc region. Which exact effector functions are elicited is a highly regulated process that lets the immune system tune its response to the pathogen in question and mediate different effector functions against, for example, a Gram-positive bacterium, a Gram-negative bacterium, or a virus. One determining factor in this process is the nature of the IgG antibody itself, namely, its subclass and the structure of its Fc glycosylation.

We here present the first evidence of a pathogen exploiting this regulatory mechanism by specifically altering IgG Fc glycosylation in vivo during the clinical course of an infection. By
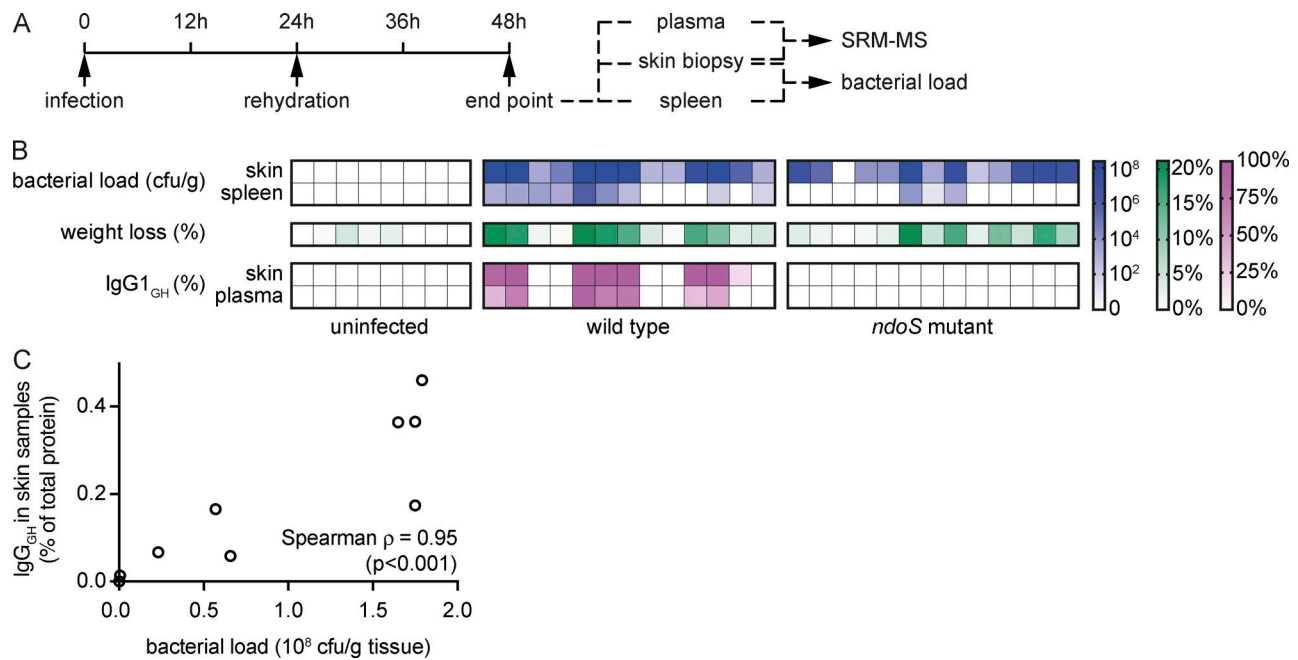
Figure 5. **EndoS leads to IgG glycan hydrolysis in a mouse model of GAS infection. (A)** Experimental setup for the infections of immunologically naive mice. 9-wk-old female C57BL/6 mice were infected subcutaneously in the flank with GAS AP1, an *ndoS* mutant, or PBS. The animals were rehydrated by injection of 0.5 ml saline at 24 h and sacrificed 48 h after infection. The spleen and a skin biopsy from the site of injection were taken to assess bacterial loads, and the skin sample, as well as a plasma sample, were used for analysis by SRM-MS. **(B)** Bacterial load (blue), weight loss (green), and percentage of IgG1 glycan hydrolysis as determined by SRM-MS (purple) 48 h after infection. Each column corresponds to an individual animal. **(C)** Correlation between skin bacterial load and absolute amount of IgG$_{GH}$. The absolute amounts of IgG$_{GH}$ in skin homogenates 48 h after infection were determined by SRM-MS (y axis) and plotted against the bacterial load in the same samples (x axis). Correlation was determined according to Spearman.

implementing a targeted proteomics approach (SRM), we were able to study the effects of EndoS on IgG antibodies during natural infections in human patients. We were able to detect and absolutely quantify IgG$_{GH}$s in a subclass-specific manner directly from a variety of very complex patient samples. With only minimal amounts of sample required and detection limits <0.5 ng, this method is far superior to any other techniques used to measure IgG glycan hydrolysis to date. With this, we were able to quantitatively address the effects of EndoS on a patient IgG population during streptococcal infections. While a slight preference of EndoS toward IgG1 has been reported (Trastoy et al., 2014), we did not observe any subclass specificity in any of the patient samples (Table S3). Our results indicate that at the site of infection, IgG is turned over quickly and constantly replenished from the circulation, and IgG glycan hydrolysis is detectable only as long as bacterial load is high and EndoS is continuously secreted. Due to the much larger amount of IgG in circulation compared with the infected tissue and the increased dilution of the enzyme further away from the site of infection, effects on the systemic IgG pool in circulation were much harder to detect and therefore rarer. Only in the most severe cases of invasive infections (septic shock) could glycan hydrolysis be observed systemically. This systemic IgG glycan hydrolysis was long-lasting, with approximately half of the IgG$_{GH}$s still present after 12 d. This is comparable to what has been observed in rabbits or mice when injected with recombinant EndoS (Collin et al., 2008; Benkhoucha et al., 2012).

In both of our patient sets, only a portion of the patient samples showed detectable levels of IgG$_{GH}$. In part, this might be due to some GAS isolates expressing only very low levels of EndoS. In vivo glycan hydrolysis was not associated with *covR/S* mutation or any specific *emm* type in the GAS isolates. Indeed we detected it in infections with ≥8 different *emm* types. All publicly available GAS genome sequences contain an *ndoS* or an *ndoS*-like gene (Sjögren et al., 2013), but expression of the EndoS protein differs greatly between different GAS isolates. However, the fact that IgG glycan hydrolysis correlates to disease severity both in tonsillitis and invasive disease indicates that, due to analytical limitations, we might not be able to detect EndoS-mediated IgG glycan hydrolysis in samples from patients suffering from less severe infections. This is true especially for the GAS sepsis patient samples. Apart from two exceptions, we were only able to study IgG in blood plasma and therefore were unable to address potential perturbations of the local IgG pool at site of infection in more detail. Indeed, among the sickest patients in each cohort, the percentage of samples with detectable IgG$_{GH}$ was considerably higher. While studying the activity of EndoS during GAS tonsillitis, we also observed a considerable amount of IgG glycan hydrolysis in some of our control samples. We speculate that this was due to enzymatic activities of the oral microbial flora, especially oral streptococci, which are known to express a large number of glycoside hydrolases (Nord et al., 1973). This is supported by the fact that IgG glycan hydrolysis was not detectable after antibiotic treatment.
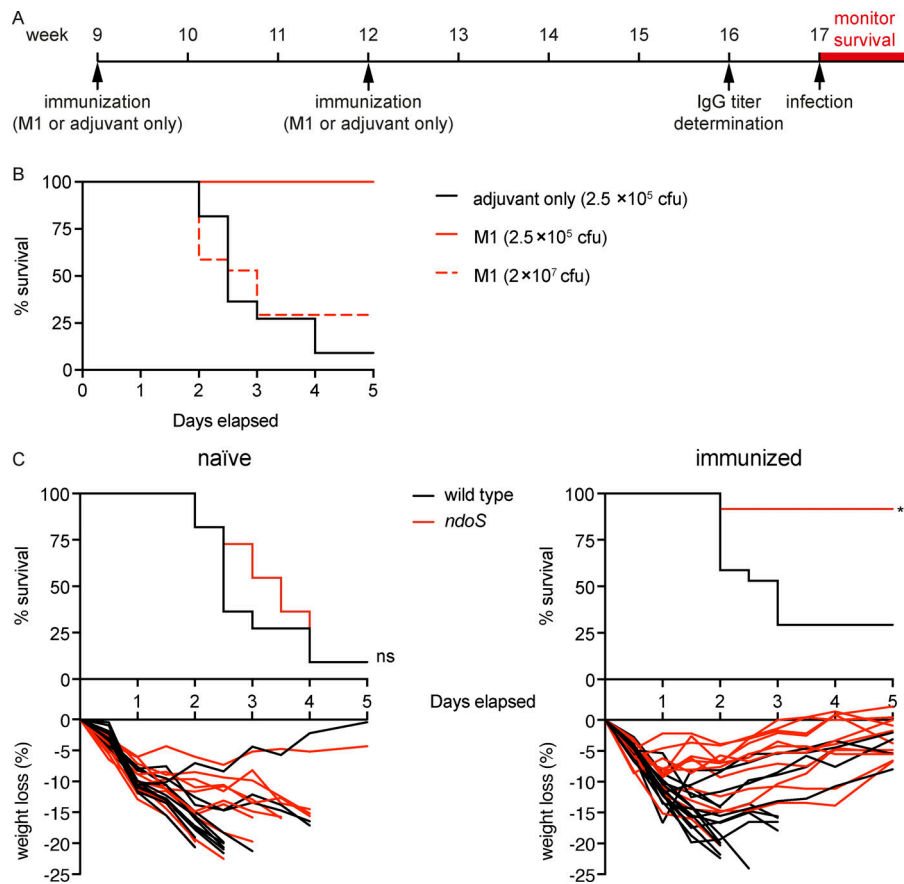
Figure 6. **EndoS confers a selective advantage in a mouse model of GAS infection. (A)** Experimental setup for the immunization with M1 and subsequent infection of mice. 9-wk-old female C57BL/6 mice were injected with purified M1 protein or adjuvant only and received a second dose at 12 wk of age. After 4 wk, the anti-M1 IgG response was assessed by ELISA, and the animals were infected subcutaneously 1 wk later. **(B)** Mice were immunized by two injections with M1 protein (red lines) or mock-immunized with adjuvant only (black line). 5-d survival was monitored after infection with GAS AP1 at a low dose (2.5 × 10⁵ CFU, unbroken lines) or a high dose (2 × 10⁷ CFU, dashed line). **(C)** Upper panels: Survival of M1-immunized (right) and mock-immunized (left) animals after infection with either GAS AP1 wild type (black) or ndoS mutant (red). Mice were monitored twice daily for survival for a period of 5 d. Curves were compared using a Mantel–Cox test (not significant [ns], P > 0.05; **, P < 0.01). Lower panel: Changes in body weight of mice infected with AP1 wild type (black) or *ndo*S mutant bacteria (red line). Each line depicts an individual animal.

While we were able to show that IgG glycan hydrolysis takes place during human GAS infection, the functional consequences of this process could not be deduced directly from the patient data. Removal of the Fc glycan by EndoS has previously been shown to impair both Fc receptor interaction and complement activation in vitro (Collin et al., 2002; Lux et al., 2013). While EndoS has been speculated to contribute to GAS virulence, all studies showing this to date had to resort to either addition of recombinant EndoS or overexpression (Collin et al., 2002; Sjögren et al., 2011) to see any effect. Thus, the conditions under which endogenous EndoS is expressed, active, and able to confer a selective advantage to the bacteria remained unclear. EndoS expression is highly regulated, and while the regulatory network responsible remains obscured, it has been shown to involve both transcriptional regulation by CcpA (catabolite control protein A) and weakly by CovR/S (control of virulence two-component system; Shelburne et al., 2010), as well as post-translational regulation through proteolysis by SpeB (Allhorn et al., 2008b). The *covR* mutant strain AP1 used in this study is a moderate to high producer of EndoS, with in vitro levels comparable to many of the clinical isolates used in this study (for example, Fig. 3 C). However, it also produces high amounts of SpeB, which, after autoproteolytic activation, degrades EndoS (this phenomenon could also be seen with some of the clinical isolates as exemplified in Fig. 3). It has been elucidated that the *covR/S* wild-type strain 5448 is much less virulent in mice than its animal passaged counterpart (that acquires *covR/S* mutations) or the AP1 strain (Fiebig et al., 2015). Transcriptomic

studies have shown that EndoS expression is repressed during growth in rich medium (Shelburne et al., 2008; such as the standard Todd-Hewitt broth) and is not induced until the bacteria reach stationary phase (Bao et al., 2015). This means that most standard assays used to study streptococcal virulence factors such as incubating log-phase bacteria with phagocytic cells and IgG (or the classic Lancefield assay; Lancefield, 1957) are ill suited to address the role of EndoS or similar secreted immunomodulatory activities. This might constitute a major shortcoming, for example, in analysis of protective effects of IgGs in vaccination studies, potentially resulting in overestimation of vaccine efficacy.

We used our characterization of IgG glycan hydrolysis in vivo to set up relevant model systems to address the contribution of EndoS to GAS pathogenesis. Based on our findings on IgG glycan hydrolysis during GAS tonsillitis, we tried to partly reconstitute in vitro the conditions GAS encounters on an inflamed tonsil using human saliva and serum. This prompted wild-type bacteria to secrete enough EndoS to completely hydrolyze the IgGs present and neutralize the contribution of GAS-specific IgGs to phagocytic killing by human macrophages or neutrophils in vitro. *ndoS* mutant bacteria, on the other hand, were unable to cleave the glycans from IgG and consequently exhibited a higher susceptibility to phagocytic killing. This phenotype could be reversed by externally adding recombinant EndoS. These results, together with the fact that the *ndoS* mutation had no phenotype in the absence of GAS-specific IgGs, indicates that the observed phenotype is due to deglycosylation of the

GAS-specific IgGs, which in turn impairs their ability to mediate phagocytic killing. There seems to be no general attenuation of the *ndoS* mutant, nor any benefits in glycan hydrolysis of nonspecific IgGs.

A mouse model of local skin infection leading to invasive infection showed very similar dynamics. Mice infected with *ndoS* mutant bacteria exhibited no IgG glycan hydrolysis and were significantly less likely to die from the infection than mice infected with wild-type GAS. This difference was, however, only clearly evident in the context of adaptive immunity (i.e., in animals that had been immunized with the cell wall–anchored M1 protein before infection). In agreement with the results from the phagocytosis assays and previous studies (Sjögren et al., 2011), naive mice showed a very similar susceptibility toward both wild-type and *ndoS* mutant bacteria, with no significant differences in survival, weight loss, or bacterial load in the skin. Only the bacterial burden in the spleen was slightly decreased in mice infected with *ndoS* mutant bacteria. This might point to a small degree of innate protection conferred by natural IgGs (Panda et al., 2013) that can be counteracted by EndoS.

While not generally used to treat sepsis (Norrby-Teglund et al., 2003; Alejandria et al., 2013), administration of IVIG has shown promise as a treatment for streptococcal toxic shock syndrome (Kaul et al., 1999; Darenberg et al., 2003) and necrotizing fasciitis (Kaul et al., 1997). Its mode of action is thought to involve neutralization of bacterial superantigens and inhibition of proinflammatory signaling (Andersson et al., 1994; Skansén-Saphir et al., 1994; Norrby-Teglund et al., 1996). Our data point to another reason that IVIG treatment could improve the outcome of severe streptococcal infections. EndoS-mediated glycan hydrolysis inactivates IgGs, and as shown in this study, such antibody modifications can be systemic and long-lasting and affect a considerable fraction of the patient's total IgG pool. GAS can lower functional IgG levels even further through secretion of the IgG protease IdeS (von Pawel-Rammingen et al., 2002; Karlsson et al., 2017). In such cases, IVIG in concert with antimicrobial therapy could help to quickly normalize the level of functional IgG in circulation. We observed such an effect in one patient (Fig. 3 E, patient 3).

Despite a widespread presence of anti-GAS IgGs in the population (Todd, 1932; Lancefield, 1962; O'Connor et al., 1991; Åkesson et al., 2004), it is not well understood how and when protective immunity develops after infections. Antibodies against GAS have been observed for a very long time and have shown to lead to opsonophagocytosis and killing of the bacteria in vitro (the classic Lancefield assay). Furthermore, individuals with high anti–M protein titers have been considered to be immune against infections with that M type (Wannamaker et al., 1953; Lancefield, 1959). To that end, a recent study has shown that one of the reasons that protective immunity does not develop is that, at least for skin infections, more than one episode within 3 wk is necessary for B cell memory to develop. Interestingly, while broadening the antibody repertoire after repeated infection, the anti–M protein antibodies seems to define the protection against a certain M serotype (Pandey et al., 2016). Our model is simplified, since we do not follow an immune response after infection, but rather vaccinate with purified M1 protein. Still, since the anti–M protein response seems to dominate after repeated skin infections in humans (Pandey et al., 2016), the antibody response in our model takes into account the major immunization events during infection. However, in future studies, it would be of great interest to see if EndoS also impacts reinfection after natural immunity arising from single and repeated infections.

Herein we present a possible mechanism to explain why generated anti-GAS IgGs could confer such poor protection: GAS is able to effectively neutralize the contribution of IgG to host defense through specific degradation of the IgG antibodies. We have demonstrated the dynamics of IgG glycan hydrolysis by EndoS in this study, and a recent study has also shown significant levels of IdeS-mediated IgG proteolysis during GAS infections in vivo (Karlsson et al., 2017). This makes GAS a very proficient evader of IgG–mediated immunity, with potential implications for the treatment of severe GAS infections. It could also be of importance in future research into the immune response to GAS as well as in the continuing efforts at development of an effective vaccine against the pathogen. Finally, immune evasion through modification of IgG glycosylation might not be restricted to GAS, and enzymes similar to EndoS can be found in many other pathogenic species such as *Enterococcus faecalis* (Collin and Fischetti, 2004) and *Streptococcus pneumoniae* (Muramatsu et al., 2001) as well as other non-group A streptococci (Flock et al., 2012; Shadnezhad et al., 2016). Indeed, an EndoS homologue from *Streptococcus equi* (Flock et al., 2012) proved to be a protective antigen in a vaccination trial in mice, pointing toward its importance for the infection process. Bacterial modulation of IgG glycosylation might therefore be a more widespread phenomenon that warrants further study.

Materials and methods

Bacterial strains

S. pyogenes strains used in the study are as follows: AP1, from the Collection of the World Health Organization Collaborating Center for Reference and Research on Streptococci (Prague, Czech Republic), serotype M1, CovSΔD319-S500; AP1ΔndoS, strain AP1 lacking the *ndoS* gene (Collin and Olsén, 2001); AP1ΔspeB, strain AP1 lacking the *speB* gene (Collin and Olsén, 2001); MC25, strain AP1 lacking the cell wall anchor of M1 protein, secretes M1 to the medium (Collin and Olsén, 2000); 5448, serotype M1 originally isolated from a patient with necrotizing fasciitis, *covR/S* wild type (Chatellier et al., 2000); and 5448ΔndoS, strain 5448 lacking the *ndoS* gene (Sjögren et al., 2011). The whole genomes of AP1 and 5448 have been sequenced (Fiebig et al., 2015).

Patient samples

Tonsillar swabs (*n* = 54; ESwab Liquid Amies) were obtained from patients (>8 yr old) seeking clinical care because of a sore throat at the primary health care clinics at Laurentiikliniken and Skåne University Hospital (SUS), both in Lund, Sweden. GAS tonsillitis was diagnosed by rapid strep test (antigen detection) and routine bacterial culturing. A follow-up tonsillar swab sample (3–5 d later) was taken from a subset of patients (*n* = 5)

treated with antibiotics (Table S3). Wound swabs from the local infection site of patients clinically diagnosed with GAS sepsis and necrotizing fasciitis were obtained from SUS (n = 4) during surgical intensive care (Table S3). Patient swab samples were transported on dry ice before storage at –80°C. The patient plasma samples were part of a larger cohort collected at the Clinic for Infectious Diseases or the Intensive Care Unit at Lund University Hospital between 2005 and 2015. All human samples were obtained with informed consent and with the approval of the local ethics committee (see Ethical considerations).

Sample preparation for MS
Proteins from the swab samples were extracted and homogenized in water using a bead-beater (Fastprep-96; MP-Biomedicals). 0.625 µl plasma or 50 µg protein from swabs or skin homogenates were prepared for MS analysis using the Smart-Digest Kit (Thermo Fisher Scientific). Samples were denatured at 90°C followed by digestion for 3.5 h at 70°C. The peptides were reduced using 50 mM tris(2-carboxyethyl)phosphine, alkylated with 100 mM iodoacetamide, and finally purified using SOLAµ HRP plates (Thermo Fisher Scientific). The peptide samples were dried in a vacuum centrifuge and dissolved in 100 µl of 50 mM sodium acetate buffer (pH 5) containing 50 mU *Thermatoga maritima* α-fucosidase (Megazymes). After incubation at 70°C for 14 h, the samples were purified a second time on SOLAµ HRP plates and dried in a vacuum centrifuge.

SRM-MS
Peptide samples were dissolved in 2% acetonitrile and 0.2% formic acid, and AQUA peptides (Thermo Fisher Scientific HeavyPeptide QuantPro; Table S2) were spiked in. The amount of peptide standards was adjusted so that the ratio of light to heavy signal fell within the interval 0.1 to 10. Samples corresponding to 1 µg of protein were analyzed by SRM-MS using a TSQ Vantage triple quadrupole mass spectrometer coupled to an Easy-nLC II system (both Thermo Fisher Scientific) equipped with a PicoChip column (PCH7515-105H354-FS25; New Objective). Data were acquired with a spray voltage of 1,500 V, 0.7 full width at half maximum, on both quadrupoles and a dwell time of 10 ms. Assays for all the nonglycopeptides were obtained from published studies (Malmström et al., 2016; Karlsson et al., 2017), while glycopeptide assays were developed as described (Lange et al., 2008). Assay setup, empirical collision energy optimization, and data analysis were done using Skyline (Maclean et al., 2010a; MacLean et al., 2010b). The analyzed transitions are listed in Table S1.

Determination of detection limits
Human IgG subclass reference serum NOR-1 (NordicMUBio) was used to create standard samples for method calibration and determination of detection limits. For a fully glycan-hydrolyzed sample, the serum was incubated with 50 µg/ml recombinant EndoS at 37°C for 16 h. Both treated and untreated serum samples were prepared for MS analysis separately as described above. Peptides were dissolved in 2% acetonitrile and 0.2% formic acid at a concentration of 1 µg/µl and spiked with AQUA IgG glycopeptides. The EndoS-treated sample was further spiked

with AQUA IgG peptides. Three separate dilution series were prepared by serially diluting the EndoS-treated sample with peptides from the untreated sample. Finally, peptides samples corresponding to 1 µg of protein from each dilution were analyzed by SRM-MS. From this dataset, detection limits for each peptide were determined separately using the following equations:

$$LoB = mean_{blank} + 1.645(SD_{blank}) \qquad (1)$$

and

$$LoD = \left[LoB + 1.645 \left(SD_{low-concentration\ sample} \right) \right], \qquad (2)$$

where *LoB* represents limit of blank and *LoD* represents limit of detection. Untreated samples were used to determine LoB according to Eq. 1. The first dilution with a concentration above LoB was used as the low-concentration sample for LoD determination with Eq. 2. A lower limit of quantification was defined as two times the LoD, and in all further experiments, measured amounts below the lower limit of quantification were considered as being 0. As the concentrations of all four IgG subclasses in serum NOR-1 have been determined by the manufacturer, we could also use this dataset to calibrate the quantification and correct for incomplete digestion and sample loss during preparation. For each data point above LoD, and with a light-to-heavy ratio between 0.1 and 10, conversion factors were determined by dividing the known IgG subclass concentrations with the measured light-to-heavy ratios. These conversion factors were averaged (Table S2) and were used to determine absolute amounts from measured light-to-heavy ratios in all further experiments with human samples. The same procedure was followed when the assay for murine IgG1 was developed. The standard sample there was a monoclonal mouse IgG1 (MA-69; BioLegend) that was treated with recombinant EndoS and spiked into human plasma as a background proteome.

SDS-PAGE and lectin blot
IgG was purified using Protein G (Ab SpinTrap; GE Healthcare). Samples were separated on SDS-PAGE (Mini-protean TGX stain-free gels, 4–15% acrylamide; Bio-Rad), imaged using a ChemiDoc MP imaging system (Bio-Rad), and transferred to low fluorescent polyvinylidene fluoride (PVDF) membranes using the Transblot Turbo kit (Bio-Rad). Membranes were blocked for 1 h in lectin buffer (10 mM Hepes, pH 7.5, 150 mM NaCl, 0.01 mM MnCl₂, 0.1 mM CaCl₂, and 0.1% [vol/vol] Tween 20) followed by incubation with 5 µg/ml fluorescein-labeled LCA lectin (Vector Laboratories). After extensive washing in lectin buffer, the membranes were imaged using the ChemiDoc MP Imager.

Analysis of EndoS and SpeB expression in vitro
AP1, AP1ΔndoS, AP1ΔspeB, and the GAS clinical isolates were grown overnight at 37°C, 5% CO₂ in C medium (0.5% [wt/vol] Proteose Peptone No. 2 [Difco] and 1.5% [wt/vol] yeast extract [Oxoid] dissolved in CM buffer [10 mM K₂PO₄, 0.4 mM MgSO₄, and 17 mM NaCl, pH 7.5]). The cultures were pelleted, and the supernatants were sterile filtered (Millex-GP filter unit 0.22 µm; Millipore). Proteins were precipitated from the supernatants with 5% TCA and analyzed by SDS-PAGE under reducing

conditions. Proteins were transferred to PVDF membranes using the Trans-Blot Turbo equipment (Bio-Rad) according to the manufacturer's instructions. Membranes were blocked with 5% (wt/vol) blotting-grade blocker (Bio-Rad) in PBS with Tween 20, followed by incubation with EndoS or SpeB rabbit antiserum (Collin and Olsén, 2000, 2001), another wash, and incubation with a secondary antibody (goat anti-rabbit HRP-conjugated antibody; Bio-Rad). The membranes were developed using Clarity Western ECL substrate (Bio-Rad) and visualized with the ChemiDoc MP Imager.

Analysis of *emm* and *covR/S* sequences

emm sequences of the GAS clinical isolates were analyzed according to protocols published by the CDC and compared with a database of known *emm* sequences using the tool on the CDC website (https://www2a.cdc.gov/ncidod/biotech/strepblast.asp). The *covR/S* operon was sequenced as previously described (Walker et al., 2007) and compared with published sequences of the same serotype.

In vitro tonsillitis model
Preparation of saliva
Saliva from healthy volunteers was collected in the morning after extensive brushing of the teeth. The saliva was centrifuged (20 min, 20,000 g), sterile filtered (Steriflip GP 0.22 μm; Millipore), and either used directly or kept at –20°C until use.

Preparation of PMNs
20 ml blood was collected into EDTA blood collection tubes (BD Bioscience), and PMNs were isolated using PolyMorphPrep (Axis-shield) according to the manufacturer's recommendations. After counting, the cells were diluted into Roswell Park Memorial Institute (RPMI) medium and seeded at 50,000 cells/well into a 96-well plate.

Preparation of MDMs
Peripheral blood mononuclear cells were isolated from leukocytes of healthy anonymous donors provided by the Lund University Hospital. Red blood cells were removed by centrifugation on Lymphoprep (Fresenius Norge), and recovered peripheral blood mononuclear cells were washed to remove platelets. Monocytes were isolated using a magnetic cell separation system with anti-CD14 mAb–coated microbeads (Miltenyi Biotec). CD14-positive monocytes were seeded into 12-well plates at 5 × 10^5 cells/well and differentiated into macrophages by culture in complete RPMI 1640 medium (Gibco) supplemented with 10% heat-inactivated human AB$^+$ serum, 50 nM β-mercaptoethanol (Gibco), penicillin-streptomycin (Sigma-Aldrich), and 40 ng/ml M-CSF (Peprotech) at 37°C under a humidified 5% CO_2 atmosphere for 6 d. Medium was replaced on day 2, and on day 4, cells were washed with PBS and the medium was replaced with antibiotic-fee medium. The cells were further incubated until day 6 when the infection experiments took place.

Killing assays
GAS 5448 and an isogenic *ndoS* mutant (Sjögren et al., 2011) were grown overnight in THY medium (Todd–Hewitt broth

supplemented with 0.2 % yeast extract) at 37°C and 5% CO_2, diluted 1:10 into fresh medium, and allowed to grow to mid-log phase (OD 0.4). Cultures were diluted 1:50 into 1 ml of saliva, incubated for 2 h at 37°C and 5% CO_2, and diluted again (1:20) into 1 ml fresh saliva (supplemented with 5% serum and 0.5 μg/ml recombinant EndoS where suitable). After 20 h at 37°C and 5% CO_2, the bacteria were diluted 1:10 into RPMI medium and used to infect PMNs or MDMs at a multiplicity of infection of 2. After 30-min (for PMNs) or 2-h (for MDMs) incubation at 37°C and 5% CO_2, the cells were lysed using double-distilled H_2O (for PMNs) or 0.025% Triton X-100 (for MDMs), and the number of surviving bacteria was determined by plating on THY agar plates.

Analysis of EndoS expression in vitro
AP1, the *ndoS* mutant, and the GAS clinical isolates were grown in C medium (37°C and 5% CO_2) overnight and normalized to the same OD_{620} using fresh C medium. Bacteria were pelleted by centrifugation, and the supernatants were filtered (Millex-GP filter unit 0.22 μm). Proteins were precipitated from the supernatants with 5% TCA and analyzed by SDS-PAGE under reducing conditions. Proteins were transferred to PVDF membranes using the Trans-Blot Turbo kit (Bio-Rad) according to the manufacturer's instructions. Membranes were blocked with 5% (wt/vol) blotting-grade blocker (Bio-Rad) in PBS with Tween 20, followed by incubation with EndoS (Collin and Olsén, 2001) or SpeB (Collin and Olsén, 2000) antiserum. The membranes were washed, followed by incubation with a secondary antibody (goat anti-rabbit HRP-conjugated antibody; Bio-Rad). The membranes were developed using Clarity Western ECL substrate (Bio-Rad) and visualized with the ChemiDoc MP Imager.

Mouse infections
Acute infection model of GAS in naive C57BL/6J mice
GAS AP1 and *ndoS* mutant were grown to logarithmic phase in Todd–Hewitt broth (37°C, 5% CO_2). Bacteria were washed and resuspended in sterile PBS. 2–3 × 10^5 CFU of AP1 ($n = 13$) or *ndoS* mutant ($n = 13$) were injected subcutaneously into the flank of 9-wk-old female C57BL/6J mice (Scanbur/Charles River Laboratories). Control mice were injected with PBS ($n = 8$). Mice were rehydrated subcutaneously with saline 24 h after infection. Body weight and general symptoms of infection were monitored regularly. Mice were sacrificed 48 h after infection, and organs (blood, spleens, and skin) were harvested to determine the degree of bacterial dissemination and IgG glycan hydrolysis.

M1 immunization and survival study
9-wk-old female C57BL/6J mice were injected subcutaneously with M1 protein on days 0 and 21 (10 μg/dose), purified as previously described (Collin and Olsén, 2001; Påhlman et al., 2006). The protein was administered as a 50:50 solution of M1:adjuvant (TiterMax Gold) in a 50-μl volume. Control mice were similarly injected with PBS:adjuvant solution. Serum was collected at day 49, and anti-M1 titers were measured by ELISA as previously described (Shannon et al., 2007) with a goat anti-mouse HRP-conjugated secondary antibody at 1:5,000 (Bio-Rad).

Naegeli et al.
Immune evasion through IgG glycan hydrolysis

Journal of Experimental Medicine   1626
https://doi.org/10.1084/jem.20190293

Immunized and control mice were infected subcutaneously into the flank with 2×10^7 CFU of the AP1 ($n = 17$) or *ndoS* mutant ($n = 12$) at day 56. Mice were rehydrated subcutaneously with saline 24 h after infection. Weight and general symptoms of infection were monitored every 12 h during the acute phase of the infection, and then every 24 h until termination of the study at 5 d after infection. Animals displaying weight loss exceeding 20% (≤72 h after infection) or 15% (>72 h after infection) were considered moribund and sacrificed.

Statistics
All statistical analyses were preformed using GraphPad Prism 7. Phagocytic killing assays were analyzed using one-way ANOVA followed by Tukey's multiple comparison test. IgG hydrolysis data were analyzed using a Mann–Whitney U test or a Kruskal–Wallis test in combination with Dunn's multiple comparison test (when more than two datasets were compared). Correlation was determined according to Spearman, and survival data were analyzed using a Mantel–Cox test.

Ethical considerations
All animal use and procedures were approved by the local Malmö/Lund Institutional Animal Care and Use Committee, ethical permit number M115-13. Collection and analysis of human throat swabs and plasma samples was approved by the regional ethics committee (Regionala Etikprövningsnämden i Lund, permit numbers 2005/790, 2015/314, and 2016/39).

Data availability
The MS analysis files from Skyline underlying Figs. 1 D, 2 B, 3 (B, D, and E), and 5 B are available on PanoramaWeb (https://panoramaweb.org/endos.url).

Online supplemental material
Fig. S1 shows IgG SRM assay calibration. Fig. S2 shows anti-M1 IgG response in donor sera for phagocytosis assays. Table S1 shows an overview of all the SRM transitions analyzed in this study. Table S2 shows SRM detection limits and conversion factors. Table S3 shows patient and bacterial isolate information.

Acknowledgments

References

Ackerman, M.E., M. Crispin, X. Yu, K. Baruah, A.W. Boesch, D.J. Harvey, A.-S. Dugast, E.L. Heizen, A. Ercan, I. Choi, et al. 2013. Natural variation in Fc glycosylation of HIV-specific antibodies impacts antiviral activity. *J. Clin. Invest.* 123:2183–2192. https://doi.org/10.1172/JCI65708

Addona, T.A., S.E. Abbatiello, B. Schilling, S.J. Skates, D.R. Mani, D.M. Bunk, C.H. Spiegelman, L.J. Zimmerman, A.-J.L. Ham, H. Keshishian, et al. 2009. Multi-site assessment of the precision and reproducibility of multiple reaction monitoring-based measurements of proteins in plasma. *Nat. Biotechnol.* 27:633–641. https://doi.org/10.1038/nbt.1546

Åkesson, P., J. Cooney, F. Kishimoto, and L. Björck. 1990. Protein H--a novel IgG binding bacterial protein. *Mol. Immunol.* 27:523–531. https://doi.org/10.1016/0161-5890(90)90071-7

Åkesson, P., K.H. Schmidt, J. Cooney, and L. Björck. 1994. M1 protein and protein H: IgGFc- and albumin-binding streptococcal surface proteins encoded by adjacent genes. *Biochem. J.* 300:877–886. https://doi.org/10.1042/bj3000877

Åkesson, P., M. Rasmussen, E. Mascini, U. von Pawel-Rammingen, R. Janulczyk, M. Collin, A. Olsen, E. Mattsson, M.L. Olsson, L. Bjorck, and B. Christensson. 2004. Low antibody levels against cell wall-attached proteins of *Streptococcus pyogenes* predispose for severe invasive disease. *J. Infect. Dis.* 189:797–804. https://doi.org/10.1086/381982

Albert, H., M. Collin, D. Dudziak, J.V. Ravetch, and F. Nimmerjahn. 2008. In vivo enzymatic modulation of IgG glycosylation inhibits autoimmune disease in an IgG subclass-dependent manner. *Proc. Natl. Acad. Sci. USA.* 105:15005–15009. https://doi.org/10.1073/pnas.0808248105

Alejandria, M.M., M.A.D. Lansang, L.F. Dans, and J.B. Mantaring III. 2013. Intravenous immunoglobulin for treating sepsis, severe sepsis and septic shock. *Cochrane Database Syst. Rev.* (9):CD001090. https://doi.org/10.1002/14651858.CD001090.pub2

Allhorn, M., A.I. Olin, F. Nimmerjahn, and M. Collin. 2008a. Human IgG/Fc gamma R interactions are modulated by streptococcal IgG glycan hydrolysis. *PLoS One.* 3:e1413. https://doi.org/10.1371/journal.pone.0001413

Allhorn, M., A. Olsén, and M. Collin. 2008b. EndoS from *Streptococcus pyogenes* is hydrolyzed by the cysteine proteinase SpeB and requires glutamic acid 235 and tryptophans for IgG glycan-hydrolyzing activity. *BMC Microbiol.* 8:3. https://doi.org/10.1186/1471-2180-8-3

Alter, G., K.G. Dowell, E.P. Brown, T.J. Suscovich, A. Mikhailova, A.E. Mahan, B.D. Walker, F. Nimmerjahn, C. Bailey-Kellogg, and M.E. Ackerman. 2018. High-resolution definition of humoral immune response correlates of effective immunity against HIV. *Mol. Syst. Biol.* 14:e7881. https://doi.org/10.15252/msb.20177881

Anderson, L., and C.L. Hunter. 2006. Quantitative mass spectrometric multiple reaction monitoring assays for major plasma proteins. *Mol. Cell. Proteomics.* 5:573–588. https://doi.org/10.1074/mcp.M500331-MCP200

Andersson, U., L. Björk, U. Skansén-Saphir, and J. Andersson. 1994. Pooled human IgG modulates cytokine production in lymphocytes and

monocytes. *Immunol. Rev.* 139:21–42. https://doi.org/10.1111/j.1600-065X.1994.tb00855.x

Bao, Y.-J., Z. Liang, J.A. Mayfield, S.W. Lee, V.A. Ploplis, and F.J. Castellino. 2015. CovRS-regulated transcriptome analysis of a hypervirulent M23 strain of group A *Streptococcus pyogenes* provides new insights into virulence determinants. *J. Bacteriol.* 197:3191–3205. https://doi.org/10.1128/JB.00511-15

Benkhoucha, M., N. Molnarfi, M.-L. Santiago-Raber, M.S. Weber, D. Merkler, M. Collin, and P.H. Lalive. 2012. IgG glycan hydrolysis by EndoS inhibits experimental autoimmune encephalomyelitis. *J. Neuroinflammation.* 9:209. https://doi.org/10.1186/1742-2094-9-209

Burton, D.R. 1985. Immunoglobulin G: functional sites. *Mol. Immunol.* 22:161–206. https://doi.org/10.1016/0161-5890(85)90151-8

Burton, D.R., and R.A. Dwek. 2006. Immunology. Sugar determines antibody activity. *Science.* 313:627–628. https://doi.org/10.1126/science.1131712

Carapetis, J.R., A.C. Steer, E.K. Mulholland, and M. Weber. 2005. The global burden of group A streptococcal diseases. *Lancet Infect. Dis.* 5:685–694. https://doi.org/10.1016/S1473-3099(05)70267-X

Centor, R.M., J.M. Witherspoon, H.P. Dalton, C.E. Brody, and K. Link. 1981. The diagnosis of strep throat in adults in the emergency room. *Med. Decis. Making.* 1:239–246. https://doi.org/10.1177/0272989X8100100304

Chatellier, S., N. Ihendyane, R.G. Kansal, F. Khambaty, H. Basma, A. Norrby-Teglund, D.E. Low, A. McGeer, and M. Kotb. 2000. Genetic relatedness and superantigen expression in group A streptococcus serotype M1 isolates from patients with severe and nonsevere invasive diseases. *Infect. Immun.* 68:3523–3534. https://doi.org/10.1128/IAI.68.6.3523-3534.2000

Collin, M., and V.A. Fischetti. 2004. A novel secreted endoglycosidase from *Enterococcus faecalis* with activity on human immunoglobulin G and ribonuclease B. *J. Biol. Chem.* 279:22558–22570. https://doi.org/10.1074/jbc.M402156200

Collin, M., and A. Olsén. 2000. Generation of a mature streptococcal cysteine proteinase is dependent on cell wall-anchored M1 protein. *Mol. Microbiol.* 36:1306–1318. https://doi.org/10.1046/j.1365-2958.2000.01942.x

Collin, M., and A. Olsén. 2001. EndoS, a novel secreted protein from *Streptococcus pyogenes* with endoglycosidase activity on human IgG. *EMBO J.* 20:3046–3055. https://doi.org/10.1093/emboj/20.12.3046

Collin, M., M.D. Svensson, A.G. Sjöholm, J.C. Jensenius, U. Sjöbring, and A. Olsén. 2002. EndoS and SpeB from *Streptococcus pyogenes* inhibit immunoglobulin-mediated opsonophagocytosis. *Infect. Immun.* 70:6646–6651. https://doi.org/10.1128/IAI.70.12.6646-6651.2002

Collin, M., O. Shannon, and L. Björck. 2008. IgG glycan hydrolysis by a bacterial enzyme as a therapy against autoimmune conditions. *Proc. Natl. Acad. Sci. USA.* 105:4265–4270. https://doi.org/10.1073/pnas.0711271105

Darenberg, J., N. Ihendyane, J. Sjölin, E. Aufwerber, S. Haidl, P. Follin, J. Andersson, and A. Norrby-Teglund. StreptIg Study Group. 2003. Intravenous immunoglobulin G therapy in streptococcal toxic shock syndrome: a European randomized, double-blind, placebo-controlled trial. *Clin. Infect. Dis.* 37:333–340. https://doi.org/10.1086/376630

Dixon, E.V., J.K. Claridge, D.J. Harvey, K. Baruah, X. Yu, S. Vesiljevic, S. Mattick, L.K. Pritchard, B. Krishna, C.N. Scanlan, et al. 2014. Fragments of bacterial endoglycosidase s and immunoglobulin g reveal subdomains of each that contribute to deglycosylation. *J. Biol. Chem.* 289:13876–13889. https://doi.org/10.1074/jbc.M113.532812

Fiebig, A., T.G. Loof, A. Babbar, A. Itzek, J.J. Koehorst, P.J. Schaap, and D.P. Nitsche-Schmitz. 2015. Comparative genomics of *Streptococcus pyogenes* M1 isolates differing in virulence and propensity to cause systemic infection in mice. *Int. J. Med. Microbiol.* 305:532–543. https://doi.org/10.1016/j.ijmm.2015.06.002

Flock, M., L. Frykberg, M. Sköld, B. Guss, and J.-I. Flock. 2012. Antiphagocytic function of an IgG glycosyl hydrolase from Streptococcus equi subsp. equi and its use as a vaccine component. *Infect. Immun.* 80:2914–2919. https://doi.org/10.1128/IAI.06083-11

Hong, Q., C.B. Lebrilla, S. Miyamoto, and L.R. Ruhaak. 2013. Absolute quantitation of immunoglobulin G and its glycoforms using multiple reaction monitoring. *Anal. Chem.* 85:8585–8593. https://doi.org/10.1021/ac4009995

Karlsson, C.A.Q., S. Järnum, L. Winstedt, C. Kjellman, L. Björck, A. Linder, and J.A. Malmström. 2017. *Streptococcus pyogenes* infection and the human proteome with a special focus on the IgG-cleaving enzyme IdeS. *bioRxiv.* (Preprint posted December 2, 2017). https://doi.org/10.1101/214890

Kaul, R., A. McGeer, D.E. Low, K. Green, and B. Schwartz. 1997. Population-based surveillance for group A streptococcal necrotizing fasciitis: Clinical features, prognostic indicators, and microbiologic analysis of seventy-seven cases. Ontario Group A Streptococcal Study. *Am. J. Med.* 103:18–24. https://doi.org/10.1016/S0002-9343(97)00160-5

Kaul, R., A. McGeer, A. Norrby-Teglund, M. Kotb, B. Schwartz, K. O'Rourke, J. Talbot, and D.E. Low. The Canadian Streptococcal Study Group. 1999. Intravenous immunoglobulin therapy for streptococcal toxic shock syndrome--a comparative observational study. *Clin. Infect. Dis.* 28:800–807. https://doi.org/10.1086/515199

Lancefield, R.C. 1957. Differentiation of group A streptococci with a common R antigen into three serological types, with special reference to the bactericidal test. *J. Exp. Med.* 106:525–544. https://doi.org/10.1084/jem.106.4.525

Lancefield, R.C. 1959. Persistence of type-specific antibodies in man following infection with group A streptococci. *J. Exp. Med.* 110:271–292. https://doi.org/10.1084/jem.110.2.271

Lancefield, R.C. 1962. Current knowledge of type-specific M antigens of group A streptococci. *J. Immunol.* 89:307–313.

Lange, V., P. Picotti, B. Domon, and R. Aebersold. 2008. Selected reaction monitoring for quantitative proteomics: a tutorial. *Mol. Syst. Biol.* 4:222. https://doi.org/10.1038/msb.2008.61

Lu, L.L., A.W. Chung, T.R. Rosebrock, M. Ghebremichael, W.H. Yu, P.S. Grace, M.K. Schoen, F. Tafesse, C. Martin, V. Leung, et al. 2016. A functional role for antibodies in tuberculosis. *Cell.* 167:433–443.e14. https://doi.org/10.1016/j.cell.2016.08.072

Lux, A., X. Yu, C.N. Scanlan, and F. Nimmerjahn. 2013. Impact of immune complex size and glycosylation on IgG binding to human FcγRs. *J. Immunol.* 190:4315–4323. https://doi.org/10.4049/jimmunol.1200501

Maclean, B., D.M. Tomazela, S.E. Abbatiello, S. Zhang, J.R. Whiteaker, A.G. Paulovich, S.A. Carr, and M.J. Maccoss. 2010a. Effect of collision energy optimization on the measurement of peptides by selected reaction monitoring (SRM) mass spectrometry. *Anal. Chem.* 82:10116–10124. https://doi.org/10.1021/ac102179j

MacLean, B., D.M. Tomazela, N. Shulman, M. Chambers, G.L. Finney, B. Frewen, R. Kern, D.L. Tabb, D.C. Liebler, and M.J. MacCoss. 2010b. Skyline: an open source document editor for creating and analyzing targeted proteomics experiments. *Bioinformatics.* 26:966–968. https://doi.org/10.1093/bioinformatics/btq054

Malmström, E., O. Kilsgård, S. Hauri, E. Smeds, H. Herwald, L. Malmström, and J. Malmström. 2016. Large-scale inference of protein tissue origin in gram-positive sepsis plasma using quantitative targeted proteomics. *Nat. Commun.* 7:10261. https://doi.org/10.1038/ncomms10261

McMillan, D.J., P.A. Drèze, T. Vu, D.E. Bessen, J. Guglielmini, A.C. Steer, J.R. Carapetis, L. Van Melderen, K.S. Sriprakash, and P.R. Smeesters. 2013. Updated model of group A *Streptococcus* M proteins based on a comprehensive worldwide study. *Clin. Microbiol. Infect.* 19:E222–E229. https://doi.org/10.1111/1469-0691.12134

Muramatsu, H., H. Tachikui, H. Ushida, X. Song, Y. Qiu, S. Yamamoto, and T. Muramatsu. 2001. Molecular cloning and expression of endo-β-N-acetylglucosaminidase D, which acts on the core structure of complex type asparagine-linked oligosaccharides. *J. Biochem.* 129:923–928. https://doi.org/10.1093/oxfordjournals.jbchem.a002938

Nandakumar, K.S., B.P. Johansson, L. Björck, and R. Holmdahl. 2007. Blocking of experimental arthritis by cleavage of IgG antibodies in vivo. *Arthritis Rheum.* 56:3253–3260. https://doi.org/10.1002/art.22930

Nord, C.E., L. Linder, T. Wadström, and A.A. Lindberg. 1973. Formation of glycoside-hydrolases by oral streptococci. *Arch. Oral Biol.* 18:391–402. https://doi.org/10.1016/0003-9969(73)90163-5

Norrby-Teglund, A., R. Kaul, D.E. Low, A. McGeer, D.W. Newton, J. Andersson, U. Andersson, and M. Kotb. 1996. Plasma from patients with severe invasive group A streptococcal infections treated with normal polyspecific IgG inhibits streptococcal superantigen-induced T cell proliferation and cytokine production. *J. Immunol.* 156:3057–3064.

Norrby-Teglund, A., N. Ihendyane, and J. Darenberg. 2003. Intravenous immunoglobulin adjunctive therapy in sepsis, with special emphasis on severe invasive group A streptococcal infections. *Scand. J. Infect. Dis.* 35:683–689. https://doi.org/10.1080/00365540310015944

Nose, M., and H. Wigzell. 1983. Biological significance of carbohydrate chains on monoclonal antibodies. *Proc. Natl. Acad. Sci. USA.* 80:6632–6636. https://doi.org/10.1073/pnas.80.21.6632

O'Connor, S.P., D. Darip, K. Fraley, C.M. Nelson, E.L. Kaplan, and P.P. Cleary. 1991. The human antibody response to streptococcal C5a peptidase. *J. Infect. Dis.* 163:109–116. https://doi.org/10.1093/infdis/163.1.109

Okazaki, A., E. Shoji-Hosaka, K. Nakamura, M. Wakitani, K. Uchida, S. Kakita, K. Tsumoto, I. Kumagai, and K. Shitara. 2004. Fucose depletion from human IgG1 oligosaccharide enhances binding enthalpy and

association rate between IgG1 and FcgammaRIIIa. *J. Mol. Biol.* 336: 1239–1249. https://doi.org/10.1016/j.jmb.2004.01.007

Påhlman, L.I., M. Mörgelin, J. Eckert, L. Johansson, W. Russell, K. Riesbeck, O. Soehnlein, L. Lindbom, A. Norrby-Teglund, R.R. Schumann, et al. 2006. Streptococcal M protein: a multipotent and powerful inducer of inflammation. *J. Immunol.* 177:1221–1228. https://doi.org/10.4049/jimmunol.177.2.1221

Panda, S., J. Zhang, N.S. Tan, B. Ho, and J.L. Ding. 2013. Natural IgG antibodies provide innate protection against ficolin-opsonized bacteria. *EMBO J.* 32:2905–2919. https://doi.org/10.1038/emboj.2013.199

Pandey, M., V. Ozberk, A. Calcutt, E. Langshaw, J. Powell, T. Rivera-Hernandez, M.-F. Ho, Z. Philips, M.R. Batzloff, and M.F. Good. 2016. Streptococcal immunity is constrained by lack of immunological memory following a single episode of pyoderma. *PLoS Pathog.* 12: e1006122. https://doi.org/10.1371/journal.ppat.1006122

Peschke, B., C.W. Keller, P. Weber, I. Quast, and J.D. Lünemann. 2017. Fc-galactosylation of human immunoglobulin gamma isotypes improves C1q binding and enhances complement-dependent cytotoxicity. *Front. Immunol.* 8:646. https://doi.org/10.3389/fimmu.2017.00646

Pucić, M., A. Knezević, J. Vidic, B. Adamczyk, M. Novokmet, O. Polasek, O. Gornik, S. Supraha-Goreta, M.R. Wormald, I. Redzić, et al. 2011. High throughput isolation and glycosylation analysis of IgG-variability and heritability of the IgG glycome in three isolated human populations. *Mol. Cell. Proteomics.* 10:010090. https://doi.org/10.1074/mcp.M111.010090

Shadnezhad, A., A. Naegeli, J. Sjögren, B. Adamczyk, F. Leo, M. Allhorn, N.G. Karlsson, A. Jensen, and M. Collin. 2016. EndoSd: an IgG glycan hydrolyzing enzyme in *Streptococcus dysgalactiae* subspecies *dysgalactiae*. *Future Microbiol.* 11:721–736. https://doi.org/10.2217/fmb.16.14

Shannon, O., E. Hertzén, A. Norrby-Teglund, M. Mörgelin, U. Sjöbring, and L. Björck. 2007. Severe streptococcal infection is associated with M protein-induced platelet activation and thrombus formation. *Mol. Microbiol.* 65:1147–1157. https://doi.org/10.1111/j.1365-2958.2007.05841.x

Shelburne, S.A. III, D. Keith, N. Horstmann, P. Sumby, M.T. Davenport, E.A. Graviss, R.G. Brennan, and J.M. Musser. 2008. A direct link between carbohydrate utilization and virulence in the major human pathogen group A *Streptococcus*. *Proc. Natl. Acad. Sci. USA.* 105:1698–1703. https://doi.org/10.1073/pnas.0711767105

Shelburne, S.A., R.J. Olsen, B. Suber, P. Sahasrabhojane, P. Sumby, R.G. Brennan, and J.M. Musser. 2010. A combination of independent transcriptional regulators shapes bacterial virulence gene expression during infection. *PLoS Pathog.* 6:e1000817. https://doi.org/10.1371/journal.ppat.1000817

Shinkawa, T., K. Nakamura, N. Yamane, E. Shoji-Hosaka, Y. Kanda, M. Sakurada, K. Uchida, H. Anazawa, M. Satoh, M. Yamasaki, et al. 2003. The absence of fucose but not the presence of galactose or bisecting N-acetylglucosamine of human IgG1 complex-type oligosaccharides shows the critical role of enhancing antibody-dependent cellular cytotoxicity. *J. Biol. Chem.* 278:3466–3473. https://doi.org/10.1074/jbc.M210665200

Sjögren, J., C.Y.M. Okumura, M. Collin, V. Nizet, and A. Hollands. 2011. Study of the IgG endoglycosidase EndoS in group A streptococcal phagocyte resistance and virulence. *BMC Microbiol.* 11:120. https://doi.org/10.1186/1471-2180-11-120

Sjögren, J., W.B. Struwe, E.F.J. Cosgrave, P.M. Rudd, M. Stervander, M. Allhorn, A. Hollands, V. Nizet, and M. Collin. 2013. EndoS2 is a unique and conserved enzyme of serotype M49 group A *Streptococcus* that hydrolyses N-linked glycans on IgG and α1-acid glycoprotein. *Biochem. J.* 455: 107–118. https://doi.org/10.1042/BJ20130126

Sjögren, J., E.F.J. Cosgrave, M. Allhorn, M. Nordgren, S. Björk, F. Olsson, S. Fredriksson, and M. Collin. 2015. EndoS and EndoS2 hydrolyze Fc-glycans on therapeutic antibodies with different glycoform selectivity and can be used for rapid quantification of high-mannose glycans. *Glycobiology.* 25:1053–1063. https://doi.org/10.1093/glycob/cwv047

Skansén-Saphir, U., J. Andersson, L. Björk, and U. Andersson. 1994. Lymphokine production induced by streptococcal pyrogenic exotoxin-A is selectively down-regulated by pooled human IgG. *Eur. J. Immunol.* 24: 916–922. https://doi.org/10.1002/eji.1830240420

St Sauver, J.L., A.L. Weaver, L.J. Orvidas, R.M. Jacobson, and S.J. Jacobsen. 2006. Population-based prevalence of repeated group A β-hemolytic streptococcal pharyngitis episodes. *Mayo Clin. Proc.* 81:1172–1176. https://doi.org/10.4065/81.9.1172

Subedi, G.P., and A.W. Barb. 2015. The structural role of antibody N-glycosylation in receptor interactions. *Structure.* 23:1573–1583. https://doi.org/10.1016/j.str.2015.06.015

Subedi, G.P., and A.W. Barb. 2016. The immunoglobulin G1 N-glycan composition affects binding to each low affinity Fc γ receptor. *MAbs.* 8: 1512–1524. https://doi.org/10.1080/19420862.2016.1218586

Todd, E.W. 1932. Antigenic streptococcal hemolysin. *J. Exp. Med.* 55:267–280. https://doi.org/10.1084/jem.55.2.267

Trastoy, B., J.V. Lomino, B.G. Pierce, L.G. Carter, S. Günther, J.P. Giddens, G.A. Snyder, T.M. Weiss, Z. Weng, L.-X. Wang, and E.J. Sundberg. 2014. Crystal structure of *Streptococcus pyogenes* EndoS, an immunomodulatory endoglycosidase specific for human IgG antibodies. *Proc. Natl. Acad. Sci. USA.* 111:6714–6719. https://doi.org/10.1073/pnas.1322908111

von Pawel-Rammingen, U., B.P. Johansson, and L. Björck. 2002. IdeS, a novel streptococcal cysteine proteinase with unique specificity for immunoglobulin G. *EMBO J.* 21:1607–1615. https://doi.org/10.1093/emboj/21.7.1607

Walker, M.J., A. Hollands, M.L. Sanderson-Smith, J.N. Cole, J.K. Kirk, A. Henningham, J.D. McArthur, K. Dinkla, R.K. Aziz, R.G. Kansal, et al. 2007. DNase Sda1 provides selection pressure for a switch to invasive group A streptococcal infection. *Nat. Med.* 13:981–985. https://doi.org/10.1038/nm1612

Walker, M.J., T.C. Barnett, J.D. McArthur, J.N. Cole, C.M. Gillen, A. Henningham, K.S. Sriprakash, M.L. Sanderson-Smith, and V. Nizet. 2014. Disease manifestations and pathogenic mechanisms of Group A *Streptococcus*. *Clin. Microbiol. Rev.* 27:264–301. https://doi.org/10.1128/CMR.00101-13

Wannamaker, L.W., F.W. Denny, W.D. Perry, A.C. Siegel, and C.H. Rammelkamp Jr. 1953. Studies on immunity to streptococcal infections in man. *AMA Am. J. Dis. Child.* 86:347–348.

Wuhrer, M., J.C. Stam, F.E. van de Geijn, C.A.M. Koeleman, C.T. Verrips, R.J.E.M. Dolhain, C.H. Hokke, and A.M. Deelder. 2007. Glycosylation profiling of immunoglobulin G (IgG) subclasses from human serum. *Proteomics.* 7:4070–4081. https://doi.org/10.1002/pmic.200700289

Supplemental material
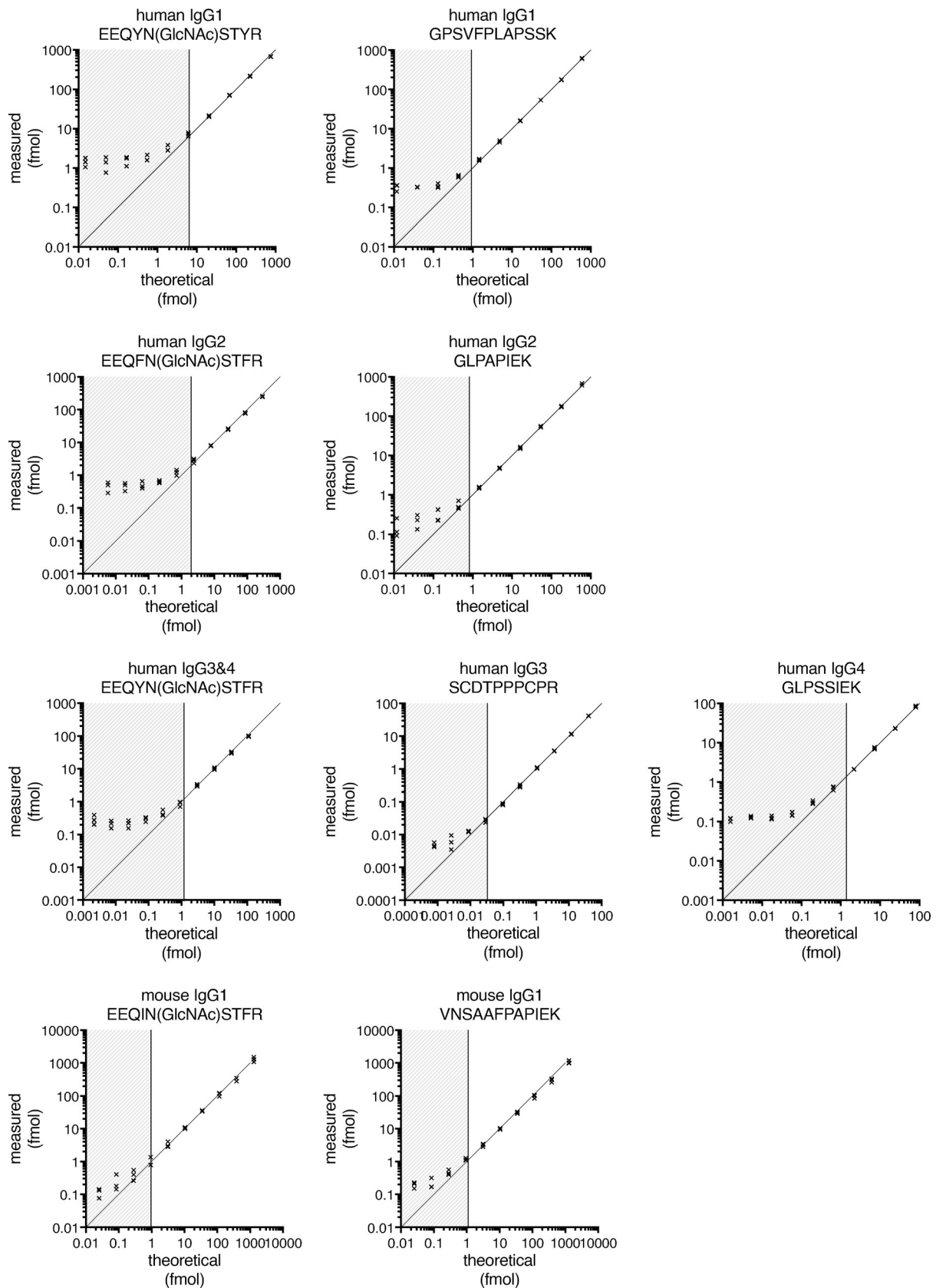
Figure S1. **IgG SRM assay calibration.** Measured amounts of each peptide are plotted against the theoretical amounts. The line and shading mark measurements below the limit of quantification.
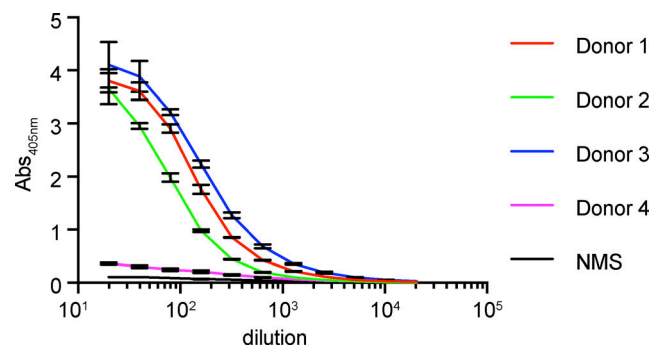
Figure S2. **Anti-M1 IgG response in donor sera for phagocytosis assays.** IgG response to M1 was determined by ELISA, and absorbance (Abs) at 405 nm in respect to serum dilution is shown. Data are presented as mean of triplicates with errors bars representing SEM. Donors 1–3 were classified as high anti-M1 response, and donor 4 as low anti-M1 response. Normal mouse serum (NMS) acted as negative control.

Table S1. **SRM assay for human and mouse IgGs**

| Protein	Peptide sequence	Isotope label	Precursor m/z	Fragment m/z	Collision energy	Ion
Human IgG1	GPSVFPLAPSSK	Light	593.83	846.47	26	y8
	GPSVFPLAPSSK	Light	593.83	699.4	18	y7
	GPSVFPLAPSSK	Light	593.83	489.27	20	y5
	GPSVFPLAPSSK	Light	593.83	418.23	20	y4
	GPSVFPLAPSSK̲	Heavy	597.83	854.49	26	y8
	GPSVFPLAPSSK̲	Heavy	597.83	707.42	18	y7
	GPSVFPLAPSSK̲	Heavy	597.83	497.28	20	y5
	GPSVFPLAPSSK̲	Heavy	597.83	426.24	20	y4
	EEQYN[GlcNAc]STYR	Light	696.80	204.09	21	GlcNAc
	EEQYN[GlcNAc]STYR	Light	696.80	843.38	21	y5
	EEQYN[GlcNAc]STYR	Light	696.80	640.19	21	y5[a]
	EEQYN[GlcNAc]STYR	Light	696.80	526.26	21	y4
	EEQYN[GlcNAc]STYR̲	Heavy	701.80	204.09	21	GlcNAc
	EEQYN[GlcNAc]STYR̲	Heavy	701.80	853.39	21	y5
	EEQYN[GlcNAc]STYR̲	Heavy	701.80	650.20	21	y5[a]
	EEQYN[GlcNAc]STYR̲	Heavy	701.80	536.27	21	y4
Human IgG2	GLPAPIEK	Light	412.75	654.38	15	y6
	GLPAPIEK	Light	412.75	557.33	15	y5
	GLPAPIEK	Light	412.75	486.29	15	y4
	GLPAPIEK	Light	412.75	276.16	15	y2
	GLPAPIEK̲	Heavy	416.75	662.40	15	y6
	GLPAPIEK̲	Heavy	416.75	565.34	15	y5
	GLPAPIEK̲	Heavy	416.75	494.31	15	y4
	GLPAPIEK̲	Heavy	416.75	284.17	15	y2
	EEQFN[GlcNAc]STFR	Light	680.80	204.09	23	GlcNAc
	EEQFN[GlcNAc]STFR	Light	680.80	974.46	15	y6
	EEQFN[GlcNAc]STFR	Light	680.80	827.39	15	y5
	EEQFN[GlcNAc]STFR	Light	680.80	510.27	21	y4
	EEQFN[GlcNAc]STFR̲	Heavy	685.81	204.09	23	GlcNAc
	EEQFN[GlcNAc]STFR̲	Heavy	685.81	984.47	15	y6
	EEQFN[GlcNAc]STFR̲	Heavy	685.81	837.40	15	y5
	EEQFN[GlcNAc]STFR̲	Heavy	685.81	520.28	21	y4
Human IgG3	SCDTPPPCPR	Light	593.75	824.41	21	y7
	SCDTPPPCPR	Light	593.75	723.36	21	y6
	SCDTPPPCPR	Light	593.75	626.31	21	y5
	SCDTPPPCPR	Light	593.75	529.26	21	y4
	SCDTPPPCPR̲	Heavy	598.76	834.42	21	y7
	SCDTPPPCPR̲	Heavy	598.76	733.37	21	y6
	SCDTPPPCPR̲	Heavy	598.76	636.32	21	y5
	SCDTPPPCPR̲	Heavy	598.76	539.26	21	y4

Naegeli et al.
Immune evasion through IgG glycan hydrolysis

Journal of Experimental Medicine   S4
https://doi.org/10.1084/jem.20190293

Protein	Peptide sequence	Isotope label	Precursor m/z	Fragment m/z	Collision energy	Ion
Human IgG4	GLPSSIEK	Light	415.73	660.36	15	y6
	GLPSSIEK	Light	415.73	563.30	15	y5
	GLPSSIEK	Light	415.73	476.27	15	y4
	GLPSSIE<u>K</u>	Heavy	419.74	668.37	15	y6
	GLPSSIE<u>K</u>	Heavy	419.74	571.32	15	y5
	GLPSSIE<u>K</u>	Heavy	419.74	484.29	15	y4
Human IgG3 and 4	EEQYN[GlcNAc]STFR	Light	688.80	204.09	25	GlcNAc
	EEQYN[GlcNAc]STFR	Light	688.80	1,118.51	14	y7
	EEQYN[GlcNAc]STFR	Light	688.80	915.32	20	y7[a]
	EEQYN[GlcNAc]STFR	Light	688.80	990.45	16	y6
	EEQYN[GlcNAc]STF<u>R</u>	Heavy	693.81	204.09	25	GlcNAc
	EEQYN[GlcNAc]STF<u>R</u>	Heavy	693.81	1,128.52	14	y7
	EEQYN[GlcNAc]STF<u>R</u>	Heavy	693.81	925.33	20	y7[a]
	EEQYN[GlcNAc]STF<u>R</u>	Heavy	693.81	1,000.46	16	y6
Mouse IgG1	VNSAAFPAPIEK	Light	622.34	872.49	20	y8
	VNSAAFPAPIEK	Light	622.34	801.45	16	y7
	VNSAAFPAPIEK	Light	622.34	654.38	20	y5
	VNSAAFPAPIEK	Light	622.34	486.29	32	y4
	VNSAAFPAPIE<u>K</u>	Heavy	626.34	880.5	20	y8
	VNSAAFPAPIE<u>K</u>	Heavy	626.34	809.46	16	y7
	VNSAAFPAPIE<u>K</u>	Heavy	626.34	662.4	20	y5
	VNSAAFPAPIE<u>K</u>	Heavy	626.34	494.31	32	y4
	EEQIN[GlcNAc]STFR	Light	663.81	204.09	20	GlcNAc
	EEQIN[GlcNAc]STFR	Light	663.81	827.39	22	y5
	EEQIN[GlcNAc]STFR	Light	663.81	624.20	24	y5[a]
	EEQIN[GlcNAc]STFR	Light	663.81	510.27	24	y4
	EEQIN[GlcNAc]STF<u>R</u>	Heavy	668.82	204.09	20	GlcNAc
	EEQIN[GlcNAc]STF<u>R</u>	Heavy	668.82	837.40	22	y5
	EEQIN[GlcNAc]STF<u>R</u>	Heavy	668.82	634.21	24	y5[a]
	EEQIN[GlcNAc]STF<u>R</u>	Heavy	668.82	520.28	24	y4

Table S1. **SRM assay for human and mouse IgGs (*Continued*)**

Protein	Peptide sequence	Isotope label	Precursor m/z	Fragment m/z	Collision energy	Ion
RT peptides	AGGSSEPVTGLADK	Light	644.82	800.45	22	y8
	AGGSSEPVTGLADK	Light	644.82	604.33	22	y6
	VEATFGVDESANK	Light	683.83	966.45	23	y9
	VEATFGVDESANK	Light	683.83	819.38	23	y8
	YILAGVESNK	Light	547.30	817.44	19	y8
	YILAGVESNK	Light	547.30	633.32	19	y6
	TPVISGGPYYER	Light	669.84	1,041.50	23	y9
	TPVISGGPYYER	Light	669.84	928.42	23	y8
	TPVITGAPYYER	Light	683.85	956.45	23	y8
	TPVITGAPYYER	Light	683.85	855.40	23	y7
	GDLDAASYYAPVR	Light	699.34	926.47	24	y8
	GDLDAASYYAPVR	Light	699.34	855.44	24	y7
	TGFIIDPGGVIR	Light	622.85	713.39	22	y7
	TGFIIDPGGVIR	Light	622.85	598.37	22	y6
	GTFIIDPAAIVR	Light	636.87	854.51	22	y8
	GTFIIDPAAIVR	Light	636.87	626.40	22	y6
	ADVTPADFSEWSK	Light	726.84	1,066.48	25	y9
	ADVTPADFSEWSK	Light	726.84	387.19	25	b4

Overview of all the SRM transitions analyzed in this study. All cysteines are carbamidomethylated. Underlined residues are heavy isotope–labeled (^{13}C and ^{15}N).
[a]Fragment ions that have undergone a neutral loss of the GlcNAc modification.

Table S2. **SRM detection limits and conversion factors**

Protein	Peptide sequence	LLoQ (fmol)	Conversion factor
Human IgG1	GPSVFPLAPSSK	1.62	1.74
	EEQYN[GlcNAc]STYR	6.41	2.15
Human IgG2	GLPAPIEK	1.45	1.76
	EEQFN[GlcNAc]STFR	1.98	1.23
Human IgG3	SCDTPPPCPR	0.16	1.64
Human IgG4	GLPSSIEK	2.38	1.72
Human IgG3 and 4	EEQYN[GlcNAc]STFR	1.19	1.74
Mouse IgG1	VNSAAFPAPIEK	1.11	1.29
	EEQIN[GlcNAc]STFR	0.96	3.47

Lower limits of quantification (LLoQs) and conversion factors are given for all the peptides analyzed by SRM in this study. The conversion factor denotes the ratio between the measured amounts and the amounts of each peptide spiked in.

Table S3 is provided online as a separate Excel file and lists patient and bacterial isolate information.